Available online at www.sciencedirect.com
ScienceDirect
International Journal of Coal Geology 68 (2006) 171–195
International Journal of COAL GEOLOGY
www.elsevier.com/locate/ijcoalgeo

# Metamorphism of mineral matter in coal from the Bukit Asam deposit, south Sumatra, Indonesia

Rita Susilawati [1], Colin R. Ward *

*School of Biological, Earth and Environmental Sciences, University of New South Wales, Sydney 2052, Australia*

Received 28 September 2005; received in revised form 6 February 2006; accepted 8 February 2006
Available online 19 May 2006

**Abstract**

The coal of the Miocene Bukit Asam deposit in south Sumatra is mostly sub-bituminous in rank, consistent with regional trends due to burial processes. However, effects associated with Plio–Pleistocene igneous intrusions have produced coal with vitrinite reflectance up to at least 4.17% (anthracite) in different parts of the deposit. The un-metamorphosed to slightly metamorphosed coals, with $Rv_{max}$ values of 0.45–0.65%, contain a mineral assemblage made up almost entirely of well-ordered kaolinite and quartz. The more strongly heat-affected coals, with $Rv_{max}$ values of more than 1.0%, are dominated by irregularly and regularly interstratified illite/smectite, poorly crystallized kaolinite and paragonite (Na mica), with chlorite in some of the anthracite materials. Kaolinite is abundant in the partings of the lower-rank coals, but is absent from the partings in the higher-rank areas, even at similar horizons in the same coal seam. Regularly interstratified illite/smectite, which is totally absent from the partings in the lower-rank coals, dominates the mineralogy in the partings associated with the higher-rank coal beds. A number of reactions involving the alteration of silicate minerals appear to have occurred in both the coal and the associated non-coal lithologies during the thermal metamorphism generated by the intrusions. The most prominent involve the disappearance of kaolinite, the appearance of irregularly interstratified illite/smectite, and the formation of regular I/S, paragonite and chlorite. Although regular I/S is identified in all of the non-coal partings associated with the higher-rank coals, illite/smectite with an ordered structure is only recognised in the coal samples collected from near the bases of the seams. The I/S in the coal samples adjacent to the floor of the highest rank seam also appears to have a greater proportion of illitic components. The availability of sodium and other non-mineral inorganic elements in the original coal to interact with the kaolinite, under different thermal and geochemical conditions, appears to be the significant factor in the formation of these new minerals, and distinguishes the mineralogical changes at Bukit Asam from those developed more generally with rank increases due to burial, and from the effects of intrusions into coals that were already at higher rank levels.


*Keywords:* Coal; Mineral matter; Clay minerals; Metamorphism; Igneous intrusions; X-ray diffraction; Geochemistry; Indonesia

## 1. Introduction

The Bukit Asam coalfield is located at Tanjung Enim, about 165 km from Palembang in South Sumatra Province, Indonesia (Fig. 1). The coal deposit extends over an area approximately 4 km wide and 6 km long, and is worked in three separate open-cuts: the Air Laya, Muara Tiga and Banko pits (Fig. 1). Around 10.2 Mt of

* Corresponding author. Fax: +61 2 9385 1558.
*E-mail address:* c.ward@unsw.edu.au (C.R. Ward).
[1] Present address: Directorate of Mineral Resources Inventory, Department of Mines and Energy, Jalan Soekarno Hatta No. 444, Bandung 41254, Indonesia.

0166-5162/$ - see front matter © 2006 Elsevier B.V. All rights reserved.
doi:10.1016/j.coal.2006.02.003

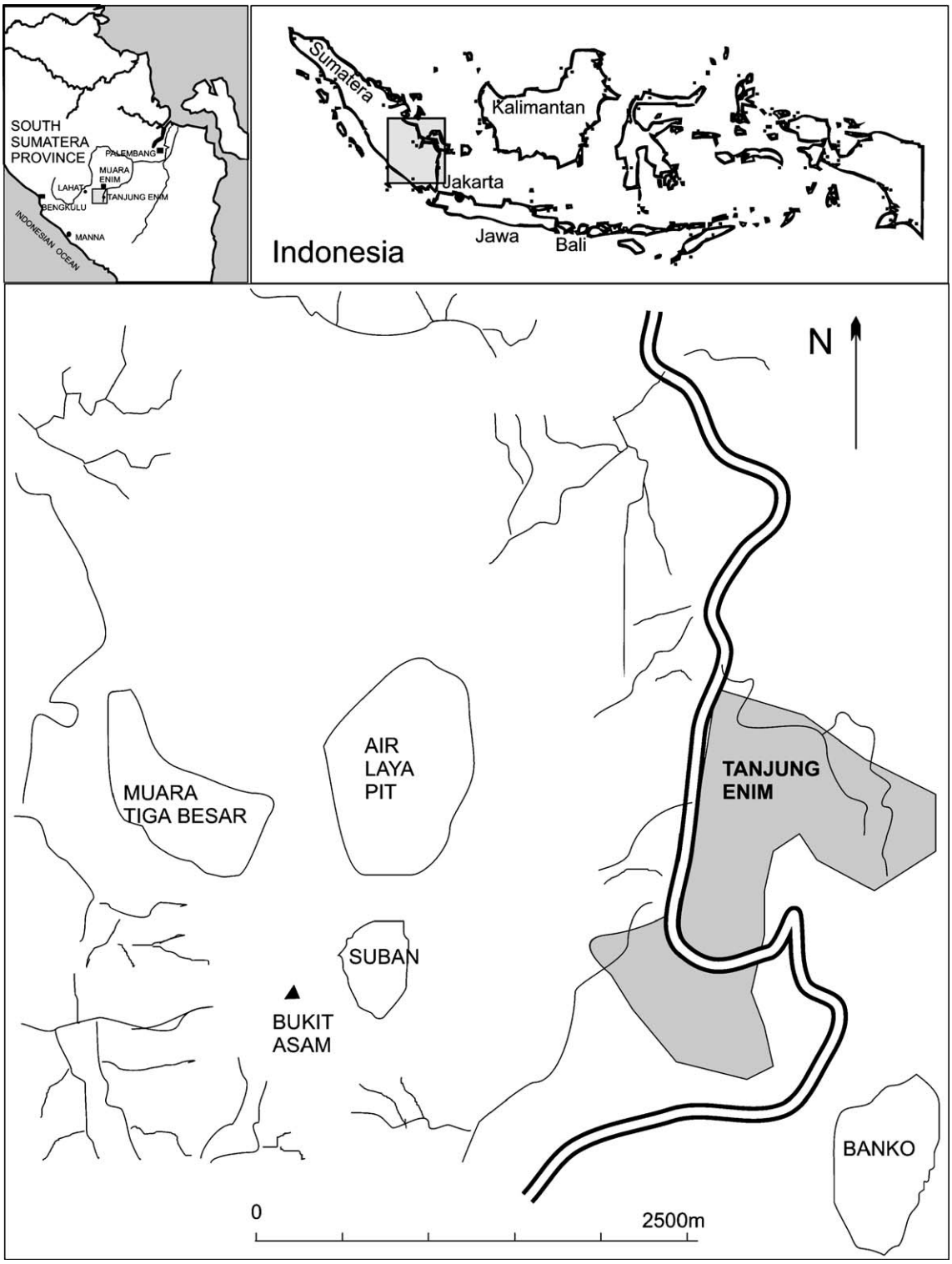


Fig. 1. Location of the Bukit Asam coalfield, South Sumatra.

coal was mined from the area in 2001, with 50% being used for domestic power production and the remainder for export markets.

The coal at Bukit Asam is mainly of sub-bituminous rank, but there are also areas within the deposit with a rank up to semi-anthracite, due to heating from nearby igneous intrusions. The Bukit Asam deposit therefore provides a good area for studying the properties of coals of very different rank within a single sedimentary succession, and indeed within individual coal seams. Although much is known about the properties of Bukit Asam coal, previous studies (e.g. Daulay, 1985; Sarangih, 1985; Daulay and Cook, 1988; Waluyo, 1992; Pujobroto, 1997) have dealt mainly with the organic matter. The present study focuses on the inorganic constituents of the coals, particularly the components making up the crystalline mineral fraction, which have not previously been studied in detail.

### 1.1. Geological setting

The Bukit Asam coalfield lies within the South Sumatra Basin, the geology of which is discussed in some detail by de Coster (1974), Haan (1976), Matasak and Kendarsi (1980), and Hutchison (1989). Stalder (1976), Waluyo (1992), Pujobroto (1997) and other authors have discussed the Bukit Asam area more specifically, with particular emphasis on the distribution and characteristics of the coal seams.

The coals at Bukit Asam are part of the Miocene Muara Enim Formation (Fig. 2), formed during the regressive phase of the Neogene depositional cycle (de Coster, 1974). Individual seams are quite widespread, and have regular thickness, ash and split patterns. The regional coalification pattern was apparently controlled mainly by burial depth variations (Stalder, 1976), with a relatively constant geothermal gradient throughout the basin. Large variations in rank that are encountered in some areas, such as at Bukit Asam, are due mainly to the effect of localised igneous intrusions on the individual coal seams.

### 1.2. Coal seams

Three economic coal-bearing intervals are present at Bukit Asam: the Mangus (A) seam, the Suban (B) seam and the Petai (C) seam (Fig. 2). The Mangus seam in the main mining area, the Air Laya pit, is split into two coal seams, called the A1 and A2 seams. The Suban seam is also split into the B1 and B2 seams, but the Petai seam is not split in this part of the coal deposit.

The A1 (Upper Mangus) seam consists mainly of bright-banded coal, with interlaminated dull and bright coal near the base and a dull coaly claystone at the top (Pujobroto, 1997). The A1 seam also contains three partings of pelletoidal claystone, generally referred to as tonsteins, varying from 10 to 35 cm in thickness. Irregular bands of hard silicified coal about 10 cm thick are also found near the base of the seam. The thickness of the seam varies from 2.5 m in the higher rank intruded zone to 9.83 m in the lower rank coal area (Shell Minjbouw, 1978).

The A2 (Lower Mangus) seam is dominated by bright-banded coal, and has a thickness ranging from 4 to 13 m (Shell Minjbouw, 1978). Bands of silicified coal about 10 to 20 cm thick occur near the top of the seam, and a discontinuous blackish-brown tonstein band in the middle part of the unit.

The Upper Suban or B1 seam ranges from 5 to 14 m in thickness, and is generally devoid of persistent tonstein bands. Two layers of claystone occur in some areas, such as in the south-west of the Air Laya pit, and in other areas four claystone bands are present (Pujobroto, 1997). Sampling for the present study, however, incorporating several vertical sections of the B1 seam, only encountered one claystone band.

The Lower Suban or B2 seam is about 2 to 6 m thick, and contains one tonstein band near the middle of the seam (Pujobroto, 1997). Bright banded coal dominates the upper part, while dull-banded coal is present in the lower part.

The lowermost coal in the study area, the C (Petai) seam ranges from about 7 to 12 m in thickness. It contains four claystone bands, with individual thicknesses varying from about 5 to 15 cm. The seam also has a higher sulphur content than the other coal beds, and pyrite is often visible in the coal in hand specimen.

### 1.3. Igneous intrusions

Andesite intrusions of Plio–Pleistocene age are exposed in several parts of the Bukit Asam area, and form pronounced hills (Bukit Asam and Bukit Tapuan) southwest of the mine. Other intrusions are exposed in the Suban area. The influence of these intrusions on the coal has been investigated by Daulay (1985), Daulay and Cook (1988) and Pujobroto (1997), among others. Isorank maps for the Mangus and Suban seams, produced by Daulay and Cook (1988), are shown in Fig. 3.

Shell Minjbouw (1978) and Pujobroto (1997) both suggested that three igneous intrusions have influenced the coal seams at Bukit Asam. Shell Minjbouw (1978) identified the three intrusions as the Bukit Asam laccolith, the Bukit Tapuan dyke, and the Suban sill (Table 1), and suggested that all three were responsible for increases in coal rank in the Bukit Asam area.

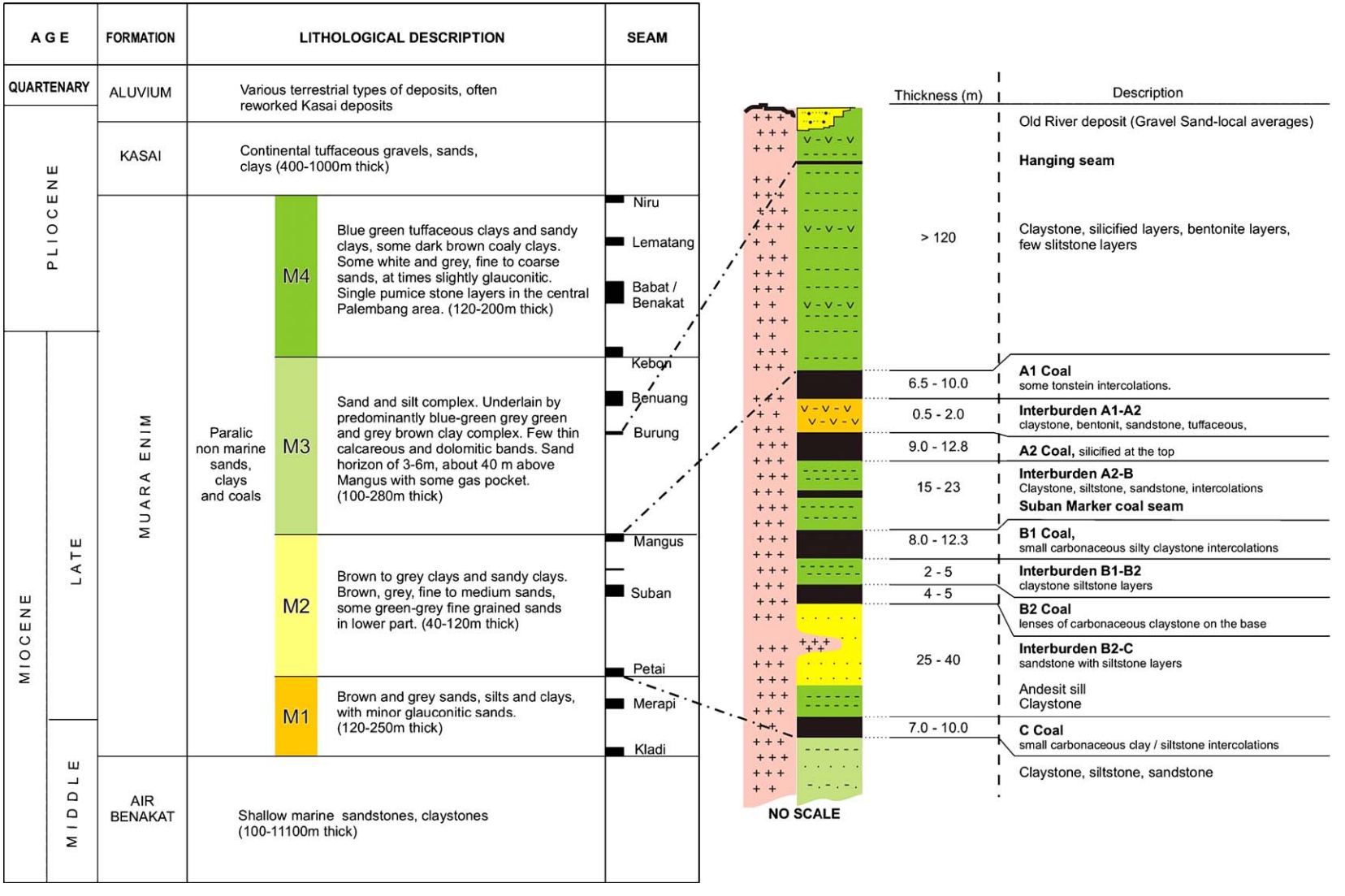


Fig. 2. Stratigraphy of the Muara Enim Formation and its coal seam nomenclature. Right side is a stratigraphic column of the Air Laya pit (modified from Shell Minjbouw, 1978).

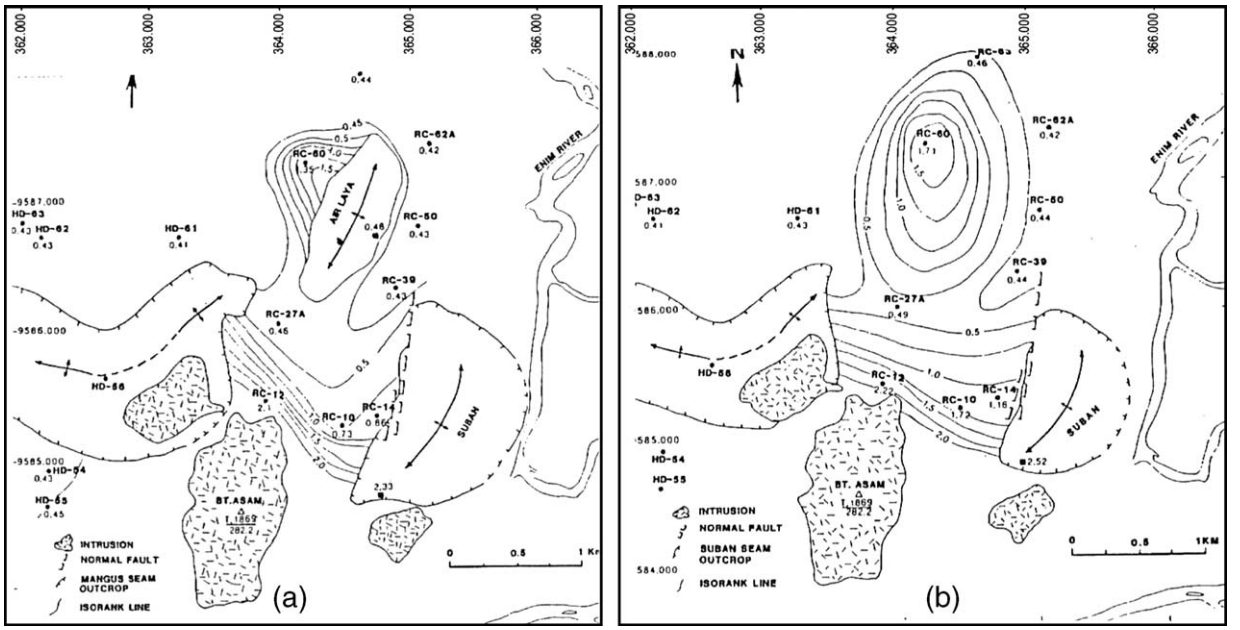


Fig. 3. Variations in rank, expressed as reflectance of vitrinite, in (a) the Mangus (A) seam and (b) the Suban (B) seam at Bukit Asam (Daulay, 1985).

Pujobroto (1997), however, interpreted the Bukit Asam laccolith as a dyke (Table 1), and did not identify the Bukit Tapuan mass as an intrusive body that influenced the coal seams.

Pujobroto (1997) also suggested that the Bukit Asam dyke was the largest igneous body, and may have been the source of magma for the other intrusions. He also noted that the influence of the Suban sill on the rank increase was greater than that of the Bukit Asam dyke, suggesting that this sill may have had a higher temperature, a larger size or a more favourable geometry than the Bukit Asam body. The Air Laya parasitic cone was identified by Pujobroto (1997) from vitrinite reflectance measurement of drill-hole samples (Fig. 4), which showed a circular pattern in the reflectance contour map around the Air Laya dome.

### 1.4. Rank of Bukit Asam coal

Pujobroto (1997) suggested that the normal level of coalification in the Bukit Asam deposit resulted in a rank corresponding to a vitrinite reflectance of about 0.40–0.46%, which is consistent with the regional rank trend for the area. Heating from the igneous bodies locally increased the maximum paleotemperature, resulting in vitrinite reflectance values that range from 0.4% to 0.5% in the unaffected areas up to at least 4.2% in the heat-affected zones.

The heating has driven off volatile matter, and in places caused the coal to lose its original structure and be transformed into a cindered coal or natural coke. Less intense heating, typically developed at greater distances from the igneous bodies, transformed parts of the seams into heat-affected coal, which has been devolatilised but still retains its physical structure. Most of the higher-rank samples included in the present study are heat-affected coals; only one sample (Anth-1, see below) represents a cindered coal.

Apart from greatly increased levels of organic maturation, it might also be expected that the changes in the coal seams associated with the igneous intrusions gave rise to significant changes in the mineral matter of the coal seams. In particular, the sudden increase in temperature associated with intrusion may have decomposed some of the minerals in the coals and re-arranged the elements present to form new mineral suites. The heating may also have introduced hot liquids into the coal-bearing formation, either from the magma itself or by remobilization of the moisture and inorganic elements in the original low-rank coal, which could then have reacted with the minerals already present to form new mineral components.

Table 1
Nomenclature for igneous intrusions in the Bukit Asam area, according to different authors

| Shell Minjbouw (1978) | Pujobroto (1997) |
|---|---|
| Bukit Asam laccolith | |
| Bukit Tapuan dyke | Bukit Asam dyke |
| Suban sill | Suban sill |
| | Air Laya parasitic cone |

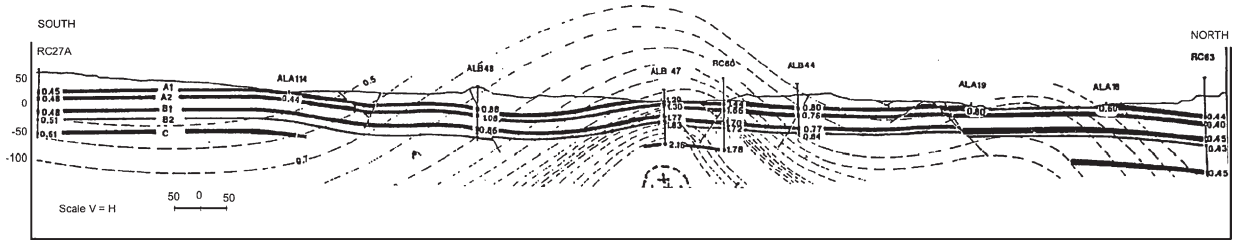


Fig. 4. Isorank lines on the western side of the Air Laya pit, suggesting the presence of the Air Laya parasitic cone (after Pujobroto, 1997).

Such changes have not previously been documented, either at Bukit Asam or in any other low-rank coal affected by widespread intrusive processes. The aim of this study was therefore to evaluate the influence of igneous intrusions on the mineralogy of the coal seams, and to identify the mechanisms that could have produced the mineralogical variations observed. The geological history of the area is quite different to that associated with intrusions into higher-rank coals, such as described by Kisch and Taylor (1966), Ward et al. (1989) and Kwiecinska et al. (1992), in that the intrusion took place into lower-rank coal beds. Much of the organic matter within lower-rank seams typically occurs as inorganic elements associated with the organic matter (Ward, 2002), and thus would be expected to behave differently during thermal metamorphism to elements occurring in the coal only as crystalline mineral phases.

## 2. Sampling and methodology

Approximately 100 samples of coal and non-coal lithologies from 15 different localities within the Bukit Asam mining area (Fig. 5) were collected for the study. The majority of the coal samples were collected, on a ply-by-ply basis, from vertical sections through individual seams in the Air Laya pit. The main suite of samples includes material from different coal beds and of different rank levels, encompassing variations in both vertical and lateral directions (Susilawati, 2004). In order to examine the lateral variations more fully, several additional coal samples were taken from the Muara Tiga, Banko and Suban pits within the Bukit Asam deposit.

Coal samples for the study were taken from the A1, A2, B1, B2 and C seams (Table 2). Because of the structure of the deposit and the distribution of mining activities, higher rank coals were not available from the A1 or A2 seams, and thus the effects of thermal metamorphism on the mineral matter were mainly evaluated from the B1, B2 and C seam samples.

The coals are generally vitrinite-rich (Table 3), with relatively low proportions of visible mineral components. Measurements on coals from the principal sections studied (Table 2) show mean maximum vitrinite reflectance values ranging from 0.45 to 4.17%. Except for one location (Suban), the actual intrusions were not exposed at the time of the study. Nevertheless, in line with a suggestion by Pujobroto (1997), vitrinite reflectance values of more than 0.5%, where encountered, were assumed to be a result of igneous intrusion effects.

Representative portions of 89 coal samples were subjected to oxygen–plasma ashing using an IPC 4-chamber asher, following procedures outlined by Standards Australia (2000). The low-temperature ash (LTA) of each sample, and also representative powdered samples of 39 additional non-coal rocks, were subjected to X-ray diffraction (XRD) analysis using CuKα radiation, with quantification of the bulk mineralogy from the resulting diffractograms using the Rietveld-based Siroquant™ data processing system (Taylor, 1991; Ward et al., 1999). Data from representative samples are given in Tables 4 and 5.

In order to identify more fully the clay minerals present in the coal and associated non-coal beds, the < 2 μm fraction was separated from six representative LTAs and six non-coal rock samples by gravitational settling, followed by separate oriented-aggregate XRD study using methods described by Griffin (1971), Moore and Reynolds (1997), and Ruan and Ward (2002). Low LTA yields and an abundance of mineral artefacts (see below) prevented wider use of the oriented-aggregate technique.

Chemical analysis of major elements in selected coal and non-coal samples was carried out by X-ray fluorescence (XRF) spectrometry, using a Philips PW2400 spectrometer. For the non-coal rocks and some of the higher-ash coal samples this was based analysis of fused borosilicate disks, prepared from calcined rock or coal ash following the method of Norrish and Chappell (1977). This was impractical for most of the coals, however, because the low percentage of mineral matter meant that insufficient ash was available from each sample to allow disk preparation. In such cases pressed powder pellets were prepared using about 9 g of dried finely crushed (<300 mesh) coal per sample, mixed intimately with a

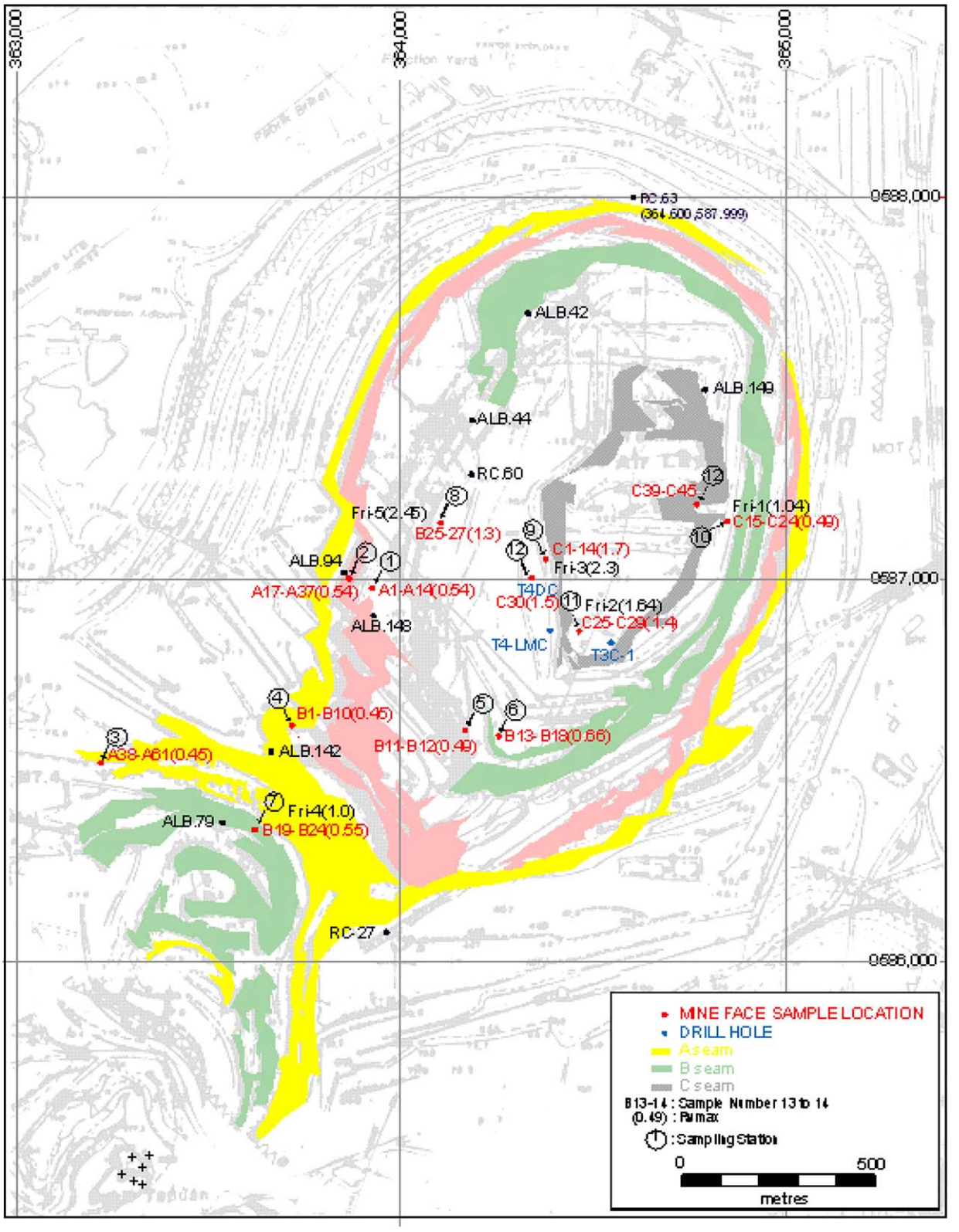


Fig. 5. Location of samples taken for the present study.

Table 2
Mean maximum vitrinite reflectance of Bukit Asam coals measured for the present study

| Sample no | Seam | Location in Air Laya pit | $Rv_{max}$ (%) | Standard deviation | Number of measurements |
|---|---|---|---|---|---|
| A5 | Mangus | 1 | 0.52 | 0.02 | 50 |
| A9 | | 1 | 0.49 | 0.02 | 30 |
| A17 | | 2 | 0.50 | 0.03 | 25 |
| A27 | | 2 | 0.57 | 0.03 | 30 |
| A30 | | 2 | 0.56 | 0.02 | 37 |
| A34 | | 2 | | | |
| A54 | | 3 | | | |
| B1 | Suban | 4 | 0.45 | 0.02 | 30 |
| B13 | | 6 | 0.67 | 0.02 | 30 |
| B19 | | 7 | 0.51 | 0.02 | 30 |
| B25 | | 8 | 1.40 | 0.03 | 30 |
| Ant-1 | | Suban | 4.17 | 0.16 | 50 |
| Ant-2 | | Suban | 2.09 | 0.04 | 25 |
| Frid-4 | | 7 | 0.54 | 0.05 | 30 |
| Frid-5 | | 8 | 2.45 | 0.17 | 50 |
| C1 | Petai | 9 | 1.71 | 0.03 | 25 |
| C15 | | 10 | 0.49 | 0.03 | 30 |
| C25 | | 11 | 1.37 | 0.03 | 25 |
| C30 | | 12 | 1.50 | 0.02 | 30 |
| Frid-1 | | 10 | 0.49 | 0.03 | 25 |
| Frid-2 | | 11 | 1.64 | 0.04 | 25 |
| Frid-3 | | 9 | 2.31 | 0.12 | 50 |
| MTB | | Muara Tiga | 0.48 | 0.02 | 30 |
| BK | | Banko | 0.48 | 0.04 | 30 |

binder made up of nine parts EMU120FD styrene co-polymer (BASF plc) and one part Ceridust 3620 micronised polyethylene wax (Hoechst). The mixture of powdered sample and binder was then compacted into an aluminium cup, pressed with a backing of boric acid powder for 1 min at a pressure of approximately 50–55 kN/m$^2$ (8000 psi).

The XRF data for major elements in the coal and non-coal rocks were expressed as weight percentages of the respective oxides (Table 6), with the values obtained from the whole-coal samples normalised so that the major element oxides usually found in coal ash totalled 100%. Potassium, and in some cases magnesium, were found to be below the detection limit, however, for many of the whole-coal samples analysed by this technique.

## 3. Mineralogy of coal and non-coal rocks

As indicated in Table 4, the coals from Bukit Asam typically have low percentages of mineral matter, with all but a few samples having less than 10% LTA. The major crystalline minerals in the coals are kaolinite and quartz, but in some samples, particularly those influenced by igneous intrusions, significant proportions of regularly and irregularly interstratified illite/smectite and the Na-mica paragonite are also present. Illite, muscovite, chlorite, boehmite, calcite, siderite and pyrite occur in some samples as minor phases. The LTA of almost all of the coal samples also contains minor to significant proportions of a range of sulphate species, such as anhydrite, bassanite, coquimbite, gypsum, jarosite, hexahydrite and alunogen. Although some (e.g. jarosite and coquimbite) may be products of pyrite oxidation, most of these probably represent artefacts formed by interaction of organic sulphur with Ca, Fe, Al, Mg and other organically associated inorganic elements during the plasma ashing process.

Table 3
Maceral composition of selected coal samples

| Sample number | Vitrinite | | | | Liptinite | | | | Inertinite | | | | | Visible minerals |
|---|---|---|---|---|---|---|---|---|---|---|---|---|---|---|
| | Tv | Dv | Gv | Total | Cut | Sb | Other | Total | Fs | Sf | Sc | Id | Total | |
| A17 | 48.6 | 40.4 | 2.2 | 91.2 | 2.0 | nd | 0.8 | 2.8 | 3.4 | 0.6 | 0.6 | 0.4 | 5.0 | 1.0 |
| A27 | 54.6 | 32.2 | 1.8 | 88.6 | 1.2 | nd | 2.4 | 3.6 | 2.0 | 2.6 | 1.4 | 0.8 | 6.8 | 1.0 |
| A32 | 45.6 | 31.4 | 0.4 | 77.4 | 2.0 | 0.4 | 1.4 | 3.8 | 10.6 | 5.0 | 0.4 | 1.2 | 17.2 | 1.6 |
| A54 | 35.6 | 37.8 | 4.0 | 77.4 | 2.8 | nd | 2.6 | 5.4 | 4.2 | 8.6 | 1.8 | 0.8 | 15.4 | 1.8 |
| B1 | 39.2 | 44.4 | 1.2 | 84.8 | 1.2 | nd | 2.2 | 3.4 | 3.2 | 2.6 | 1.4 | 0.8 | 8.0 | 3.8 |
| B13 | 51.8 | 40.0 | 1.0 | 92.8 | 0.6 | 0.8 | 1.4 | 2.8 | 1.4 | 0.8 | 0.2 | 0.4 | 2.8 | 1.6 |
| Fri-4 | 44.4 | 47 | 0.8 | 92.2 | 1.8 | 0.3 | 2.3 | 4.4 | 0.6 | 0.4 | 0.8 | 0.2 | 2.0 | 1.4 |
| Fri-5 | 74.4 | 22.2 | nd | 96.6 | nd | nd | 1.6 | 1.6 | nd | nd | 0.2 | 0.8 | 1.0 | 0.8 |
| C1 | 70.0 | 21.8 | 0.4 | 93.2 | 1.4 | nd | 0.8 | 2.2 | 1.4 | 1.8 | 0.2 | 0.2 | 3.6 | 2.0 |
| C15 | 31.8 | 47.0 | 5.0 | 83.8 | 1.8 | 1.0 | 1.8 | 4.6 | 2.2 | 4.4 | 0.8 | 0.4 | 7.8 | 8.2 |
| C25 | 61.9 | 29.6 | nd | 91.5 | nd | nd | 2.3 | 2.3 | nd | 0.2 | 0.2 | Nd | 0.4 | 5.8 |
| C30 | 60.8 | 27.8 | nd | 88.6 | 2.0 | nd | 1.4 | 3.4 | nd | nd | 0.1 | 0.3 | 0.4 | 9.6 |
| MTB | 32.0 | 49.4 | 5.4 | 86.8 | 2.0 | 4.0 | 3.0 | 9.0 | 0.2 | 0.6 | 0.8 | 1.0 | 2.6 | 1.6 |
| BK | 43.4 | 42.6 | 5.0 | 91.0 | 0.4 | nd | 2.4 | 2.8 | 1.0 | 0.6 | 1.0 | 0.4 | 3.0 | 3.2 |

Tv = telovitrinite; Dv = detrovitrinite; Gv = gelovitrinite; Cut = cutinite; Sb = suberinite; Fs = fusinite; Sf = semifusinite; Sc = secretinite; Id = inertodetrinite.

### 3.1. Quartz

Quartz is usually a relatively minor component of the minerals in the coal and intra-seam non-coal samples (Tables 4 and 5); indeed, it may make up less than 1% of the LTA of some of the coal samples. In some silicified coals and some of the floor strata, however, quartz may represent more than 70% of the total mineral matter. Quartz is also a relatively abundant mineral in the inter-seam sandstone and shale beds (Table 5).

Much of the quartz in the coal samples occurs as microcrystalline infillings of cell lumens, or as infillings of cracks within the macerals. The silica in such cases may have come from diatoms and other biogenic sources in the original peat, from transformation of clay minerals, or possibly from the alteration of volcanic ash falling into the peat swamp.

At several horizons within the sequence, particularly at the top of the A2 seam and in some parts of the B1 seam, authigenic quartz forms bands and lenses of silicified coal. The bands are approximately 40 cm thick, and extend laterally over hundreds of metres. Well-preserved petrified plant stems are also present in some of these bands. Pujobroto (1997) has suggested that leaching of tuffaceous sediments immediately above the A2 seam was the source of the silica required for the formation of these silicified coal horizons, with subsequent crystallisation as the silica-saturated solutions permeated the coalifying plant tissues beneath (cf. Sykes and Lindqvist, 1993).

The silica polymorph trydimite, distinguished by XRD peaks at 4.11, 2.99 and 2.32 Å, has also been identified in the LTA of some coals from the A and B seams. The trydimite is mostly found in coal samples taken from close to pyroclastic clay partings, and it is possible that silica released by alteration of glass, feldspar and other components in the pyroclastic sediment may have been re-precipitated in the pores of the peat to form the trydimite mineral.

### 3.2. Kaolinite

Kaolinite is present in all of the coal samples (Table 4). It dominates most of the lower rank coals, making up almost the entire clay fraction in the majority of the lower-rank samples studied. It is also the dominant mineral in the tonstein-like partings that occur within the lower-rank seams.

The XRD pattern indicates that the kaolinite in the lower-rank coals is largely well ordered (Fig. 6a), although in some samples, particularly those from the lower parts of the individual seams, it includes a significant proportion of more poorly ordered material. Kaolinite is not as abundant in the mineral matter of the higher rank or heat-affected coals ($Rv_{max}$ >1.0%), and there is a tendency for the proportion of kaolinite to decrease as the rank of the coal increases. The kaolinite in the higher-rank coals is also more disordered than in the lower-rank materials (Fig. 6b).

SEM-EDX analysis indicates that the kaolinite the coal generally occurs as broken plates and aggregates (Fig. 7a). It may be present as layers, lenticles and lenses, as encrustations on the sulphides and organic matter, or as finely dispersed particles in different maceral components. The mode of occurrence suggests that the kaolinite was formed in the original peat deposit by authigenic processes. Kaolinite in the study area is also found infilling cleats and other fractures, and in some instances is present as a matrix associated with crystalline pyrite and quartz.

### 3.3. Interstratified illite/smectite

Interstratified illite/smectite (I/S) is present in the LTA isolated from most of the higher rank coal samples, and in the associated intra-seam claystone bands. It is not, however present in significant proportions in the LTA of the lower-rank coal samples, or in the intra-seam non-coal materials associated with the lower-rank parts of the Bukit Asam deposit.

Where it does occur, the I/S in the coals is usually an irregularly interstratified material, with diffraction peaks at 11.7, 9.36 and 5.04 Å in oriented-aggregate samples after ethylene glycol treatment (Fig. 8a) that collapse to a 10 Å series after heating to 400 °C. In the non-coal samples and some of the LTAs, however, the glycol-treated oriented-aggregate XRD pattern has peaks at around 29, 12.2 and 5.1 Å (Fig. 8b), which, as indicated by Moore and Reynolds (1997) and other authors, suggests a stacking regularity and development of a superlattice structure similar to that of rectorite.

The type of ordering in mixed-layer clays is commonly expressed by the *reichweite* (reach back) value, which expresses the probability, for a given layer of type A, that the next layer will be of type B (Moore and Reynolds, 1997). Three *reichweite* values are commonly used to identify the degree of ordering in I/S and other mixed-layer clays: $R=0$, representing random ordering with no adjoining layer dependency; $R=1$, representing an ordered structure with closest-adjoining layer only dependency; $R=3$, representing ordered material with non-closest adjoining layer dependency.

Table 7 shows the estimated illite percentage and *reichweite* ordering in the I/S of representative coal and

Table 4
Mineralogy of LTA obtained from selected coal samples (minerals weight percent of LTA)

| Sample no | Seam | Location | Thickness (m) | $Rv_{max}$ (%) | LTA (%) | Quartz | Kaolinite | I/S | Illite | Chlorite | Paragonite | Muscovite | Calcite |
|---|---|---|---|---|---|---|---|---|---|---|---|---|---|
| *Sub-bituminous coals* | | | | | | | | | | | | | |
| A-17 | A-1 | 2 | 1.75 | 0.51 | 0.06 | 28.5 | 45.9 | | | | | | |
| A19 | A-1 | 2 | 1.25 | | 0.02 | 3.6 | 84.8 | | | | | | |
| A27 | A-2 | 2 | 1.00 | 0.57 | 1.99 | 69.3 | 4.9 | | | | | | 1.2 |
| A32 | A-2 | 2 | 1.00 | | 2.90 | 4.4 | 34.4 | | | | | | 2.9 |
| B1 | B-1 | 4 | 1.50 | 0.45 | 7.20 | 10.6 | 80.4 | | | | | | |
| B4 | B-1 | 4 | 1.10 | | 6.60 | 3.2 | 67.5 | | | | | | 0.5 |
| B11 | B-1 | 5 | Grab | 0.62 | 2.50 | 0.9 | 76.0 | | | | | | |
| B12 | B-1 | 5 | Grab | | 6.00 | 0.4 | 77.5 | | | | | | |
| B13 | B-2 | 6 | 1.20 | 0.66 | 4.20 | 4.2 | 87.8 | | | | | | |
| B14 | B-2 | 6 | 1.30 | | 3.20 | 18.2 | 73.6 | | | | | | |
| B19 | B-2 | 7 | 0.65 | 0.52 | 3.00 | 1.4 | 46.0 | | | | | 12.9 | |
| B23 | B-2 | 7 | 0.85 | | 2.40 | 1.5 | 38.6 | | | | | | |
| C15 | C | 10 | 0.35 | 0.49 | 11.30 | 6.8 | 67.4 | 0.2 | | | | | |
| C20 | C | 10 | 1.40 | | 9.45 | 0.8 | 87.4 | 0.1 | | | | | |
| C23 | C | 10 | 1.00 | | 7.16 | 17.1 | 49.0 | | | | | | |
| C41 | C | 12 | 1.00 | | 5.55 | 1.6 | 66.6 | | | | | | 2.6 |
| C44 | C | 12 | 1.00 | | 3.82 | 8.6 | 70.4 | | | | | | 3.6 |
| *Higher-rank coals* | | | | | | | | | | | | | |
| B25 | B-2 | 8 | 0.30 | 1.40 | 1.30 | 15.7 | 68.5 | | | | | | |
| B27 | B-2 | 8 | 0.50 | | 2.80 | | 58.2 | 27.5 | | | | | |
| C1 | C | 9 | 0.55 | 1.70 | 15.20 | 18.9 | 7.8 | 60.2 | 7.8 | | | | |
| C6 | C | 9 | 0.60 | | 4.30 | | 15.8 | 42.6 | | | 24.3 | | |
| C10 | C | 9 | 1.00 | | 2.80 | 3.2 | 31.8 | | | | 36.8 | | |
| C26 | C | 11 | 1.00 | 1.41 | 22.70 | 22.5 | 14.4 | 39.4 | | | 4.8 | | |
| C28 | C | 11 | 0.60 | | 3.20 | 10.0 | 59.1 | | | | 19.0 | | |
| C29 | C | 11 | 0.60 | | 2.11 | 1.9 | 13.6 | 10.1 | | | 35.8 | | |
| Anth-1 | B | Suban | Grab | 4.40 | 4.40 | | | | 20.4 | 34.5 | 29.2 | | |
| Anth-2 | B | Suban | Grab | 2.20 | 7.40 | | 55.0 | 33.0 | | | 9.4 | | 0.5 |

non-coal samples, as indicated from the Δ2-theta values of the XRD patterns using the criteria of Moore and Reynolds (1997). With the exception of one sample (C9), the I/S in all of the coals appears to have around 75–90% illite and R1 to R3 ordering. On the other hand, the I/S in the non-coal rocks tends to have about 50–60% illite and a regular R1 ordering. The coal in which the I/S has R1 ordering was collected from near the base of the C seam.

The mixed-layer clay minerals typically have an irregular flaky shape under the SEM (Fig. 7b), with EDX data indicating the presence of Ca, Fe, K and Na as well as Al and Si in the individual particles. Velde (1985) has pointed out that, compared to more common I/S of equivalent smectite content, the interlayer composition of rectorite tends to be rich in Na and Ca. Chemical analysis of rocks in the present study consisting almost entirely of regular I/S (Table 8) shows that sodium is slightly higher than potassium, especially as the proportion of regular I/S increases.

Although present in no more than trace amounts in the lower-rank coals, I/S is an abundant mineral in the higher-rank coal samples. Similarly, well-ordered I/S is present in almost all of the non-coal rocks associated with the heated coals, and is absent from the rocks associated with the unheated parts of the coal deposit. Unlike similar material in the coals, which collapses only to a little under 11 Å at 400 °C (Fig. 8b), the regular I/S in the non-coal rocks collapses completely to 10 Å on heating (Fig. 8c).

### 3.4. Paragonite

Paragonite (sodium mica) has been identified in the LTA of a number of higher-rank coal samples, on the basis of strong XRD peaks at 9.67–9.7, 4.85, 4.45 and 3.20–3.25 Å (Fig. 8d). The 9.7 Å peak is clearly recognized in most XRD patterns of paragonite-bearing rocks, except where the paragonite is only a minor mineral component. The mineral's identity is further confirmed by oriented XRD patterns of the clay fractions (Fig. 8b), by SEM-EDX observations (Fig. 7c), and by the linear relationship shown when the normalised $Na_2O$ percentages indicated by the XRF data from relevant

| Siderite | Pyrite | Bassanite | Gypsum | Jarosite | Coquimbite | Hexahydrite | Alunogen | Boehmite | Sanidine | Hematite | Trydimite |
|---|---|---|---|---|---|---|---|---|---|---|---|
| | 9.8 | | | | | 11.8 | | 1.8 | | 2.0 | |
| | 0.7 | 10.9 | | | | | | | | | |
| 17.7 | | | 2.4 | | | | | 2.5 | | | |
| 3.6 | | | 4.3 | | 5.1 | 14.3 | 29.2 | 1.8 | | | |
| | | 2.6 | | | | 6.4 | | | | | |
| | | 4.3 | | | | 17.6 | 6.5 | 0.5 | | | |
| | | | 15.0 | | 6.2 | | | 1.2 | | 0.7 | |
| | | | 16.8 | | 4.3 | | | 1.0 | | | |
| | | | | | 0.4 | 7.2 | | 0.4 | | | |
| | 4.2 | 1.5 | | | 1.7 | | | | | 0.9 | |
| | | | 6.5 | | 7.9 | 6.9 | 16.2 | 2.2 | | | |
| | | | 4.4 | 6.5 | 2.3 | 46.8 | | | | | |
| | 2.4 | | | 2.4 | 9.0 | | 10.6 | | 0.8 | | |
| | | | | | 0.5 | | 11.2 | | | | |
| | tr | 1.0 | | | 0.3 | 7.3 | 25.7 | | | | |
| | 2.5 | | | | | 9.0 | 15.1 | 2.6 | | | |
| 5.6 | | | | | | 7.8 | | 4.0 | | | |
| | 1.4 | 0.9 | | | | | | | | | 13.5 |
| | 7.4 | 6.6 | | | | | | | | | |
| | | | 2.0 | | 2.3 | | | | tr | | |
| | 10.9 | | 1.8 | | 2.7 | | | 2.0 | | | |
| | | | 1.2 | | 25.7 | | | 1.4 | | | |
| | 1.5 | | | 15.3 | 2.1 | | | | | | |
| | 3.0 | | 1.4 | | 0.7 | 5.9 | | 0.9 | | | |
| | 6.8 | | 11.5 | 11.6 | | | | 8.7 | | | |
| | 1.9 | | | 1.4 | 2.3 | | | 10.6 | | | |
| | | | | | | | | 2.2 | | | |

samples are plotted against the paragonite content of the mineral matter (Fig. 9).

Paragonite is an unusual mineral in coal, but is commonly present in low-grade metamorphic rocks (Frey, 1970; Chatterjee, 1973; Frey, 1978; Weaver and Broekstra, 1984). Along with regularly interstratified mica/smectite in the form of mixed layer paragonite/smectite, with 50% paragonite layers, it has nevertheless been reported in the high rank anthracites of eastern Pennsylvania (Daniels, 1992; Daniels et al., 1994). Stalder (1971), cited by Kisch (1983), has also reported the occurrence of paragonite in illitic, kaolinite-free tonsteins associated with upper Carboniferous meta-anthracites, and in the Hagen 1 anthracite seam in a well off the Ems estuary, Germany.

The paragonite at Bukit Asam is only present in the higher-rank (heat-affected) coal samples. Paragonite is identified in samples of the C seam that have $Rv_{max}$ values of 1.3–1.4%, and in anthracites in the B seam that have $Rv_{max}$ values of 2.4–4.2%. The occurrence of paragonite at Bukit Asam coals is therefore thought to be related to the thermal metamorphism of the seams. Its presence, however, is restricted to the coals; unlike the interstratified illite/smectite, paragonite has not been identified in any of the intra-seam non-coal samples.

### 3.5. Illite and muscovite

Illite in the Bukit Asam samples is mostly found as part of the mixed layer illite/smectite minerals. A significant proportion of separate illite, characterised by a *d* (001) spacing of 10 Å, especially after ethylene glycol treatment, has been identified in a silicified coal sample from a low-rank coal area (sample B22, Table 5), and in one of the anthracite samples (Anth-1, Table 4) collected near an intrusive contact. Illite is also present in trace proportions in a few other coal and intra-seam non-coal samples.

Muscovite has also been found in some of the coal and intra-seam sediment samples (Table 4), identified by two characteristically intense peaks at 9.9 Å (001) and 3.3 Å (003), and by a relatively weak peak at 5 Å (002). Its presence may also be indicated by poorly defined peaks at 10 and 5 Å, appearing as superimposed shoulders overlapping with the mixed layer clay and/or paragonite XRD peaks.

Table 5
Mineralogy (minerals weight % of selected non-coal strata (∗=rectorite-like structure)

| Sample no | Description | Thickness (m) | Interval | Coal rank | Location | Quartz | Kaolinite | I/S | Illite | Chlorite | Muscovite | Calcite | Siderite | Pyrite | Bassanite | Gypsum | Jarosite | Hexahydrite |
|---|---|---|---|---|---|---|---|---|---|---|---|---|---|---|---|---|---|---|
| *Intra-seam non-coal strata* | | | | | | | | | | | | | | | | | | |
| A18 | Tonstein | 0.2 | A-1 | Sub-bit | 2 | 12.1 | 87.9 | | | | | | | | | | | |
| A20 | Tonstein | 0.15 | A-1 | Sub-bit | 2 | 3.2 | 95 | | | | | | | 1.8 | | | | |
| A26 | Shale | Top | A-2 | Sub-bit | 2 | 14.9 | 85.1 | | | | | | | | | | | |
| A31 | Tonstein | 0.1 | A-2 | Sub-bit | 2 | | 100.0 | | | | | | | | | | | |
| B2 | Claystone | 0.1 | B-1 | Sub-bit | 4 | 26.8 | 73.2 | | | | | | | | | | | |
| B8 | Floor | | B-1 | Sub-bit | 4 | 3.3 | 96.8 | | | | | | | | | | | |
| B16 | Claystone | 0.1 | B-2 | Sub-bit | 6 | 12.4 | 85.6 | | | | | 0.3 | | | | | | |
| B20 | Claystone | 0.1 | B-2 | Sub-bit | 7 | 12.1 | 87.9 | | | | | | | | | | | |
| B22 | Silicified coal | 0.15 | B-2 | Sub-bit | 7 | 50.3 | 35.1 | | 14.5 | | | | | | | | | |
| B24 | Shale | floor | B-2 | Sub-bit | 7 | 100.0 | | | | | | | | | | | | |
| C16 | Claystone | 0.20 | C | Sub-bit | 10 | 6.9 | 93.1 | | | | | | | | | | | |
| C19 | Claystone | 0.09 | C | Sub-bit | 10 | 11.0 | 85.1 | | | | | | 3.0 | 0.9 | | | | |
| C21 | Claystone | 0.10 | C | Sub-bit | 10 | 8.6 | 91.4 | 0.2 | | | | | | | | | | |
| B26 | Silicified coal | 0.15 | B-2 | Bit | 8 | 1.5 | 57.7 | 40.2 | | | | | | | | | 0.7 | |
| C2 | Claystone | 0.18 | C | Bit | 9 | | | 75.6* | | | | | | 24.4 | | | | |
| C4 | Claystone | 0.07 | C | Bit | 9 | | | 99.5* | 0.2 | | | | | | | | | |
| C7 | Claystone | 0.09 | C | Bit | 9 | 5.5 | | 94.2* | | | | | | 0.3 | | | | |
| C12 | Claystone | 0.05 | C | Bit | 9 | | | 66.3 | | 33.7 | | | | | | | | |
| C14 | Shale | floor | C | Bit | 9 | 47.4 | 20.4 | 29.2 | | | | | 3.1 | | | | | |
| C25 | Shale | Top | C | Bit | 11 | 42.4 | 26.5 | 9.2 | | | | 1.6 | | 6.6 | 1.4 | 2.1 | | 10.3 |
| C27 | Claystone | 0.2 | C | Bit | 11 | | 7.8 | 92.0 | | | | 0.7 | | | | | | |
| *Non-coal rocks in interburden strata* | | | | | | | | | | | | | | | | | | |
| A23 | Tuffaceous clay | | A-1:A-2 | | | 48.9 | 40.3 | 10.9 | | | | | | | | | | |
| A15 | Sandstone | | A-1:A-2 | | | 65.8 | 27.5 | 1.4 | | | | | 1.1 | | | 4.2 | | |
| B9 | Claystone | | B-1:B-2 | | | 40.1 | 48.5 | 9.0 | | | | tr | | 2.4 | | | | |
| B10 | Mudstone | | B-1:B-2 | | | 25.7 | 69.1 | – | | | 4.6 | 0.6 | | | | | | |
| BC-2 | Sandstone | | B:C | | | 40.3 | 29.5 | 28.2 | | | | | | 2.0 | | | | |

Table 6
Chemical analysis of selected coal and non-coal samples by XRF techniques

| Sample | $SiO_2$ % | $Al_2O_3$ % | $Fe_2O_3$ % | CaO % | MgO % | $Na_2O$ % | $K_2O$ % | $TiO_2$ % |
|---|---|---|---|---|---|---|---|---|
| *Sub-bituminous coals* | | | | | | | | |
| A-17 | 53.28 | 30.70 | 11.10 | 2.44 | bld | 0.76 | bld | 1.73 |
| A19 | 23.65 | 36.35 | 19.62 | 12.50 | bld | 5.19 | bld | 2.69 |
| A27 | 34.71 | 6.47 | 41.96 | 10.98 | bld | 4.12 | bld | 1.76 |
| A32 | 22.57 | 45.14 | 16.93 | 9.72 | bld | 3.61 | bld | 2.04 |
| B4 | 28.14 | 35.87 | 7.51 | 21.64 | 0.22 | 4.48 | bld | 2.13 |
| B11 | 40.03 | 45.94 | 3.85 | 3.71 | bld | 3.03 | bld | 3.44 |
| B12 | 49.92 | 45.84 | 1.02 | 1.34 | bld | 0.64 | bld | 1.23 |
| B13 | 55.79 | 39.47 | 1.51 | 1.51 | bld | 0.92 | bld | 0.79 |
| B14 | 52.28 | 38.00 | 3.77 | 2.01 | bld | 2.54 | bld | 1.40 |
| B19 | 22.06 | 36.03 | 17.81 | 16.80 | 1.82 | 3.24 | bld | 2.23 |
| B23 | 18.35 | 17.41 | 24.68 | 29.11 | 2.53 | 5.38 | bld | 2.53 |
| C15 | 44.14 | 36.51 | 16.30 | 1.10 | bld | 1.23 | bld | 0.72 |
| C20 | 42.31 | 45.28 | 7.35 | 2.93 | bld | 1.55 | bld | 0.58 |
| C23 | 49.57 | 34.13 | 8.19 | 3.86 | 0.12 | 2.38 | bld | 1.76 |
| C41 | 33.94 | 37.71 | 9.58 | 7.11 | 2.36 | 2.63 | bld | 6.68 |
| C44 | 36.70 | 36.20 | 6.20 | 12.60 | bld | 8.10 | bld | 0.20 |
| C41 | 33.94 | 37.71 | 9.58 | 7.11 | 2.36 | 2.63 | bld | 6.68 |
| C44 | 36.70 | 36.20 | 6.20 | 12.60 | bld | 8.10 | bld | 0.20 |
| *Bituminous coals* | | | | | | | | |
| C1 | 48.67 | 30.25 | 13.78 | 1.03 | 1.21 | 3.02 | 0.57 | 1.47 |
| B25 | 48.01 | 28.36 | 9.20 | 9.70 | bld | 2.24 | bld | 2.49 |
| C6 | 30.78 | 32.92 | 22.91 | 3.66 | 0.21 | 8.76 | bld | 0.76 |
| C10 | 40.35 | 36.15 | 10.44 | 3.86 | bld | 7.40 | bld | 1.81 |
| C26 | 44.16 | 24.44 | 15.25 | 11.65 | 0.46 | 1.62 | 1.26 | 1.16 |
| C28 | 45.69 | 38.50 | 9.08 | 1.89 | bld | 3.97 | bld | 0.87 |
| Anth-1 | 37.38 | 42.21 | 5.01 | 6.70 | 0.75 | 6.91 | bld | 1.04 |
| Anth-2 | 46.48 | 45.56 | 2.33 | 2.29 | bld | 2.49 | bld | 0.84 |
| *Intra-seam non-coal strata* | | | | | | | | |
| A18 | 57.96 | 38.49 | 0.90 | 0.28 | 0.37 | 0.28 | 0.36 | 1.35 |
| A20 | 53.31 | 43.85 | 0.89 | 0.24 | 0.27 | 0.07 | 0.17 | 1.20 |
| A26 | 39.80 | 23.90 | 33.30 | 0.40 | 0.52 | 0.49 | 0.92 | 0.67 |
| A31 | 54.20 | 42.99 | 0.85 | 0.29 | 0.35 | 0.19 | 0.25 | 0.87 |
| B2 | 59.62 | 32.01 | 1.35 | 0.98 | 1.00 | 1.19 | 0.78 | 3.06 |
| B8 | 54.76 | 42.15 | 0.60 | 0.25 | 0.39 | 0.34 | 0.41 | 1.11 |
| B16 | 57.01 | 39.98 | 0.65 | 0.24 | 0.30 | 0.37 | 0.32 | 1.13 |
| B20 | 57.85 | 39.01 | 0.65 | 0.24 | 0.41 | 0.40 | 0.32 | 1.12 |
| B22 | 97.36 | 0.37 | 0.79 | 0.14 | 0.35 | 0.72 | 0.21 | 0.05 |
| B24 | 69.60 | 22.78 | 3.50 | 0.13 | 0.70 | 0.42 | 1.87 | 1.00 |
| B26 | 52.93 | 42.62 | 0.90 | 0.35 | 0.61 | 0.39 | 0.83 | 1.38 |
| C2 | 45.75 | 31.36 | 19.65 | 0.35 | 1.01 | 0.82 | 0.51 | 0.56 |
| C4 | 54.71 | 39.61 | 1.34 | 0.59 | 0.82 | 1.16 | 0.92 | 0.85 |
| C7 | 57.95 | 34.00 | 1.68 | 0.60 | 0.96 | 1.66 | 1.00 | 2.15 |
| C12 | 55.88 | 39.23 | 1.20 | 0.51 | 0.79 | 0.86 | 0.92 | 0.61 |
| C14 | 70.65 | 22.63 | 1.77 | 0.17 | 0.95 | 0.77 | 2.09 | 0.96 |
| C16 | 55.62 | 40.03 | 1.34 | 0.28 | 0.47 | 0.45 | 0.72 | 1.09 |
| C19 | 49.71 | 36.25 | 10.79 | 0.41 | 1.15 | 0.29 | 0.38 | 1.02 |
| C21 | 55.69 | 40.47 | 1.24 | 0.22 | 0.37 | 0.27 | 0.73 | 1.01 |
| C25 | 62.89 | 23.03 | 8.55 | 0.30 | 1.06 | 0.71 | 2.55 | 0.91 |
| C27 | 54.85 | 40.69 | 1.83 | 0.23 | 0.46 | 0.41 | 0.82 | 0.70 |
| *Non-coal rocks in interburden strata* | | | | | | | | |
| A23 | 76.44 | 19.08 | 2.09 | 0.32 | 0.91 | 0.29 | 0.53 | 0.34 |
| AB1 | 83.18 | 11.89 | 2.20 | 0.17 | 0.61 | 0.50 | 0.93 | 0.52 |
| B9 | 65.13 | 25.56 | 5.16 | 0.28 | 0.85 | 0.28 | 1.74 | 0.99 |
| B10 | 62.08 | 28.75 | 4.91 | 0.28 | 0.86 | 0.35 | 1.67 | 1.09 |
| BC-2 | 64.55 | 20.01 | 8.78 | 0.49 | 2.73 | 0.65 | 1.96 | 0.82 |

### 3.6. Chlorite

Chlorite has been identified in a few samples, mainly from the distinctive 004 peak at 3.54 Å in the XRD traces (Fig. 8d). As the 001 peak (14 Å) is low, apparently below background levels, it is likely that the chlorite material in these samples represents an iron-rich chlorite phase (cf. Moore and Reynolds, 1997).

Renton (1982) notes that chlorite is an uncommon mineral in coal, probably because it is unstable in the peat-forming environment. Chlorite is only found in the LTA of the higher-rank coals, particularly the B seam anthracite sample (Anth-1, Table 4) and some of the higher-rank C seam claystone materials (Table 5). The mineral was thus probably formed in association with rank advance, possibly through the following reaction:

$$\text{Kaolinite} + (Fe^{2+}, Mg^{2+}) + Si \rightarrow \text{Fe–Mg chlorite}$$ (Sanguesa et al., 2000)

The $Fe^{2+}$ and $Mg^{2+}$ may have been derived from the organic matter, or possibly from carbonate minerals (calcite and siderite), while the Si was probably derived from quartz in the coal.

### 3.7. Boehmite

Boehmite (Al·O·OH) has been identified in the LTA of a number of coal samples from the XRD data (Fig. 8d), and its occurrence further confirmed by SEM-EDX observations. The mineral is found as a minor component of the mineral matter in both low-rank and higher-rank coals (Table 4), but is not recognised in any of the intra-seam or inter-seam non-coal strata. It is most abundant (>5% of mineral matter) in coals where the LTA has a low quartz content.

The boehmite may have been formed from the precipitation of Al released by leaching of detrital sediment, including volcanic ash, through processes such as those indicated by Ward (2002). Oxidation of the organic matter may give rise to low pH in the peat, which may in turn allow Al to be leached from the detrital aluminosilicates and transferred to other parts of the peat deposit. In the absence of silica that would otherwise

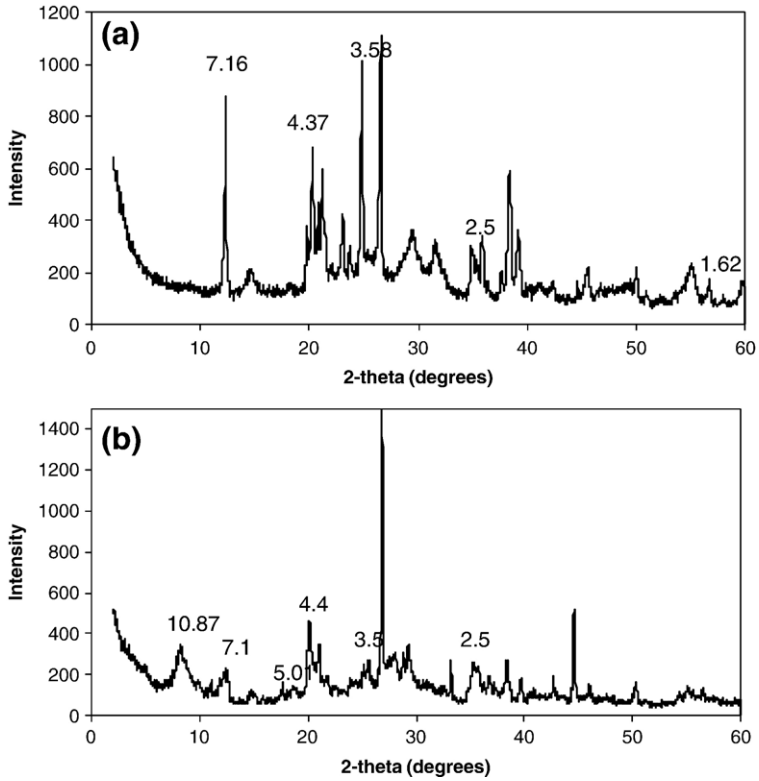


Fig. 6. X-ray powder diffractograms of representative sub-bituminous (a) and bituminous (b) coals (samples B1 and C1 in Table 4), showing abundant well-ordered kaolinite and minor quartz in the lower-rank coal, and interstratified I/S plus quartz and poorly ordered kaolinite in the higher-rank material. *d*-spacings in Å.

have formed kaolinite, the Al in this leachate may then have been precipitated to form boehmite when the pH increased, or when the leachates migrated to a higher pH area within the peat bed.

### 3.8. Pyrite, siderite and calcite

Pyrite and siderite are present as minor minerals in most Bukit Asam coal samples, with the C seam tending to have more abundant pyrite than the other coals. Petrographic analysis and SEM-EDX observations indicate that most of the pyrite in the coals is syngenetic in origin, occurring as individual crystals dispersed in the organic matter, infillings of cavities and cell lumens, and as framboids, typically 10–20 μm in diameter, made up of euhedral pyrite crystals commonly coated with fine kaolinite crusts. Some pyrite, however, occurs as veinlets and nodules, or as incrustations on vitrain bands, and may be of epigenetic origin.

Siderite appears to be randomly distributed in both the coal and non-coal lithologies, although it appears to be more abundant in the coals of the A seam (Table 4). The siderite is mainly syngenetic, occurring as fine-grained and massive accumulations or forming lenses and nodules.

Calcite is present in some of the coal and non-coal samples, but usually in only relatively minor proportions (Table 4). The mineral also has been identified in scanning electron microscope studies. Pujobroto (1997) indicates that calcite is a significant epigenetic component of heat-affected coals in the Bukit Asam area, possibly formed from Ca-rich magmatic waters that moved through the inter-seam sediments, entered the coal and precipitated in the cell lumens or cleat spaces. Most of the calcite found in the present study, however, occurs in the lower-rank coals, and little, if any, is present in the LTA of the higher-rank materials.

### 3.9. Mineral artefacts

Sulphate minerals such as gypsum ($CaSO_4{\cdot}2H_2O$), bassanite ($CaSO_4{\cdot}1/2H_2O$), hexahydrite ($MgSO_4{\cdot}6H_2O$), coquimbite ($Fe_2(SO_4)_3{\cdot}9H_2O$), jarosite ($Fe_3(SO_4)_2(OH)_6$ and alunogen ($Al_2(SO_4)_3{\cdot}17(H_2O)$ are present almost in all plasma ashes of Bukit Asam coals from the Air Laya pit. In addition, potash alum is present in plasma ash of the C seam from the Muara Tiga area.

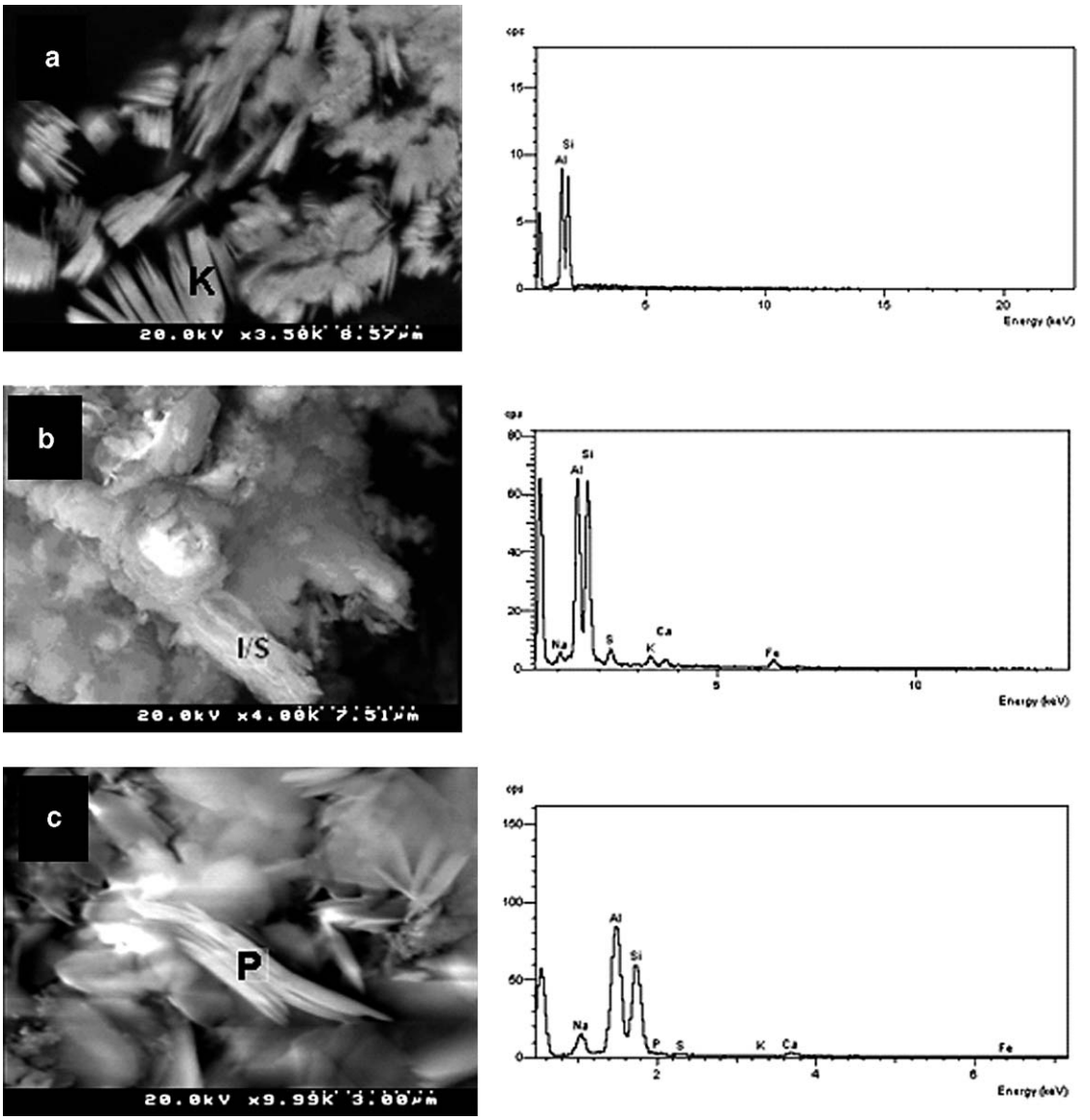


Fig. 7. SEM images and energy-dispersive X-ray (EDX) spectra of clay minerals in Bukit Asam coals: (a) kaolinite, (b) interstratified illite/smectite, (c) paragonite.

As indicated by Miller and Given (1978), Miller et al. (1979) and Ward (1991, 1992, 2002) bassanite and other sulphates in LTA residues may represent artefacts formed in the plasma ashing process by interaction between the organic sulphur in the coal and Ca, Mg and other elements occurring as inorganic components of the organic matter. The occurrence of bassanite in some cases may also reflect the dehydration during ashing of gypsum, with the gypsum being produced by reactions between calcite and sulphuric acid derived from pyrite oxidation during storage of the coal sample (Rao and Gluskoter, 1973), or precipitated by evaporation of Ca-bearing pore waters in lower-rank coal seams (Ward, 1991).

Abundant jarosite was found in the present study on the cleat surfaces at the top of the weathered C seam. Such an occurrence may represent an oxidation product of pyrite framboids originally occurring in the fresh coal, or possibly iron sulphates precipitated with evaporation of dissolved Fe in the coal's pore water.

With the exception of jarosite and coquimbite, which may represent oxidation products of pyrite, these sulphate minerals, particularly hexahydrite and alunogen, are most abundant in the lower-rank coals of the sample suite (Table 4). The lesser abundance in the higher-rank coal is consistent with progressive loss of the non-mineral inorganics from the organic matter with

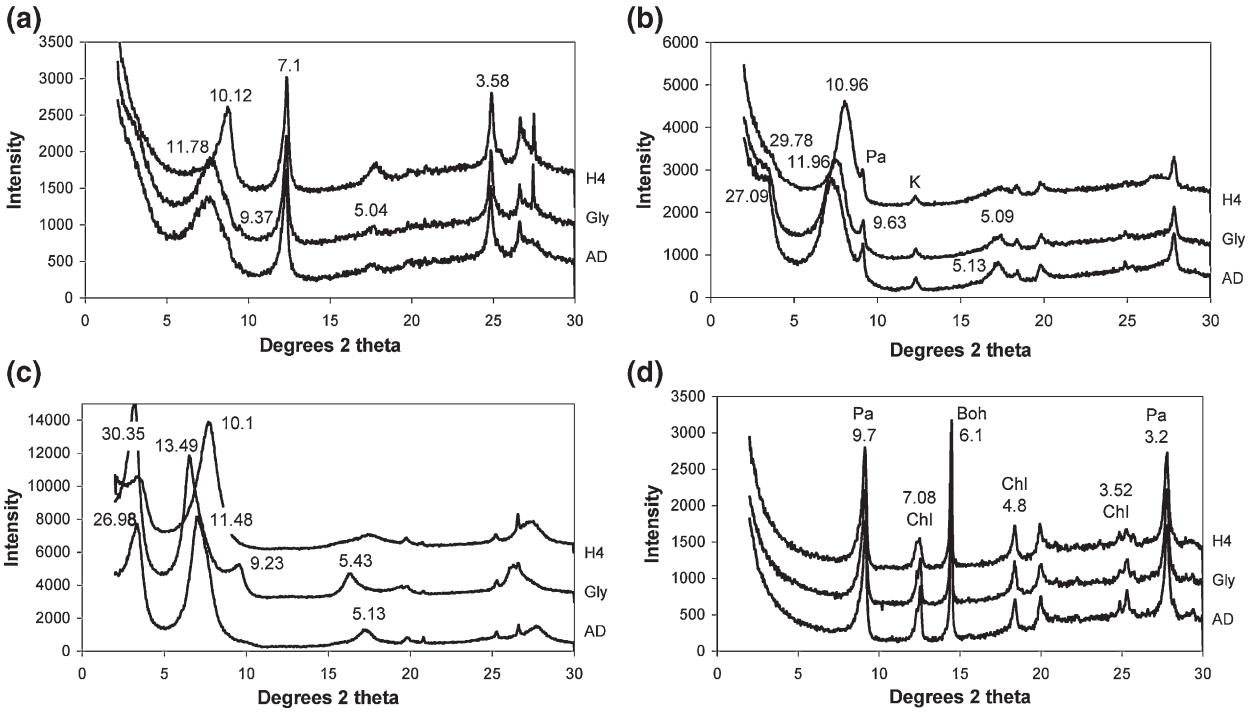


Fig. 8. Oriented-aggregate X-ray diffractograms of the clay fractions from representative LTAs and intra-seam bands: (a) LTA from bituminous coal sample C1, showing irregularly interstratified I/S; (b) LTA from bituminous coal sample C9, showing regular I/S ($d$ (001)=27–29 Å), and a paragonite peak at around 9.7 Å that remains fixed during all treatments; (c) intra-seam parting sample C7 in a bituminous coal seam, showing regular I/S ($d$ (001)=27–30 Å); (d) LTA from anthracite sample Anth-1, showing chlorite (Chl), boehmite (Boh) and paragonite (Pa). Numbers show $d$-spacings in Å; AD = air-dried; Gly = glycol-saturated; H4 = heated to 400 °C.

rank advance, as has been noted in these and other coals by Ward et al. (2003). The higher-rank samples with abundant jarosite or coquimbite are all from the C seam, which typically has higher pyrite concentrations than the other coal beds.

## 4. Mineralogical changes associated with rank advance

As indicated above, XRD and other studies clearly show that the non-artefact minerals in the LTA isolated

Table 7
Estimates of the percentage of illite in the illite/smectite of selected coal and non-coal samples, based on the °Δ2$\theta$ value of Moore and Reynolds (1997)

| Sample no | Lithology | 001/002 | | 001/002 | | °Δ2$\theta$ | % Illite | Reichweite ordering |
|---|---|---|---|---|---|---|---|---|
| | | $d$ (Å) | °2$\theta$ | $d$ (Å) | °2$\theta$ | | | |
| B25 | Silicified coal | 9.227 | 9.549 | 5.446 | 16.278 | 6.729 | 53 | 1 |
| C1 | Coal | 9.369 | 17.565 | 5.045 | 9.432 | 8.133 | 85 | 3 |
| C2 | Claystone | 9.283 | 9.519 | 5.46 | 16.219 | 6.936 | 58 | 1 |
| C4 | Claystone | 9.088 | 9.666 | 5.402 | 16.424 | 6.758 | 55 | 1 |
| C7 | Claystone | 9.226 | 9.578 | 5.439 | 16.278 | 6.729 | 54 | 1 |
| C9 | Coal | 9.637 | 9.168 | 5.095 | 17.419 | 7.801 | 78 | 1 |
| C11 | Coal | 9.383 | 9.490 | 5.441 | 16.278 | 6.788 | 56 | 1 |
| C12 | Claystone | 9.143 | 9.666 | 5.470 | 16.190 | 6.524 | 51 | 1 |
| C13 | Coal | 9.72 | 9.110 | 5.071 | 17.478 | 8.368 | 90 | 3 |
| C14 | Shale floor | 9.340 | 9.461 | 5.327 | 16.600 | 7.139 | 62 | 1 |
| C26 | Coal | 9.34 | 9.461 | 5.078 | 17.478 | 8.017 | 83 | 3 |
| C28 | Coal | 9.742 | 9.070 | 5.171 | 17.134 | 8.064 | 83 | 3 |
| Anth 2 | Coal | | 9.110 | | 17.126 | 8.016 | 83 | 3 |

Table 8
Concentrations of sodium and potassium in clay partings of higher-rank C seam coals containing abundant rectorite-like clay

| Sample no | $Na_2O$ (%) | $K_2O$ (%) | Rectorite-like clay (%) |
|---|---|---|---|
| C2 | 0.8 | 0.6 | 75.6 |
| C4 | 1.2 | 0.9 | 99.5 |
| C7 | 1.7 | 1.0 | 94.2 |

from the higher rank coals at Bukit Asam are quite different to those of the stratigraphically equivalent lower-rank materials. The unheated or slightly heated coals, with $Rv_{max}$ values of around 0.45–0.65%, generally have a mineral assemblage made up almost entirely of well-ordered kaolinite and lesser proportions of quartz. Other minerals, such as boehmite, illite, calcite, siderite, pyrite and muscovite may also be present in some cases, but only as relatively minor constituents. The heat-affected coals, on the other hand, with $Rv_{max}$ values more than 1.0%, contain a significant proportion of interstratified illite/smectite (including an ordered variety resembling rectorite), more poorly ordered kaolinite, and, in some cases, the sodium mica mineral paragonite.

The partings in the higher-rank coals are also quite different to those in the lower-rank parts of the deposit. Kaolinite, which is abundant in the partings of the lower-rank coals, is absent from the partings in the same seams at higher rank levels. Mixed-layer illite/smectite, and particularly the regularly interstratified rectorite-like mineral, is completely absent from the partings of the lower-rank coals, but dominates the partings in the higher rank coal areas.

These differences suggest that a number of phyllosilicate reactions have occurred in the coals and associated non-coal beds in association with the thermal metamorphism induced by igneous intrusion into the originally low-rank coal seams. Because there is no significant change in the overall LTA percentages or in the overall ash chemistry, the formation of new minerals in the higher rank coals appears to represent the result of iso-chemical reactions within the mineral matter present. The most prominent of these reactions are the disappearance of kaolinite, the appearance of irregular I/S and rectorite-like regular I/S, as well as paragonite and possibly chlorite.

Kübler and Jaboyedoff (2000) have divided the physical and chemical changes in clay minerals during deep burial diagenesis of sedimentary rocks into three low temperature metamorphism zones (Fig. 10): the zone of diagenesis, the anchizone (very low grade metamorphism/sub-greenschist facies), and the epizone (low grade metamorphism/greenschist facies). Although the mineral assemblages indicated Fig. 10 are not necessarily mineral assemblages in equilibrium, comparison of the minerals in the different parts of the Bukit Asam deposit with the range of mineral occurrences in the plot suggests that the mineral assemblages and metamorphic changes observed in the coals and intra-seam materials in the present study are similar to the assemblages and changes typically developed during deep burial diagenesis and low-grade metamorphism in other types of rock strata.

### 4.1. Structural changes and disappearance of kaolinite

The development of poorly ordered kaolinite or decreasing kaolinite crystallinity in areas close to the intrusions, as observed in this study, was also observed in an intruded bituminous coal seam in Australia (Ward et al., 1989). The change in crystal ordering may reflect exposure to temperatures at which the crystal structure of originally well-ordered kaolinite is disrupted, followed by re-forming of the structure under conditions that permitted a less well-ordered kaolinite to form.

In addition to the ordering of its structure, the concentration of the kaolinite in the LTA of Bukit Asam coal also tends to decrease as the rank of the coal increases. By contrast, the concentration of mixed-layer I/S in the coal and non-coal bands tends to increase as the rank increases. The same phenomena, but involving different minerals, have also been described by Daniels (1992) in coals of the eastern Pennsylvania anthracite region. As the rank of the Pennsylvania coals increases kaolinite tends to be depleted, but the abundance of $NH_4$-illite increases.

Velde (1985) indicates that kaolinite may disappear from the clay mineral paragenesis during the burial of other sedimentary sequences and their subsequent diagenesis or metamorphism, through combination with other phases to produce mixed-layer clay minerals. The temperature and depth at which kaolinite is eliminated vary from one sequence of rocks to another (Velde, 1985;

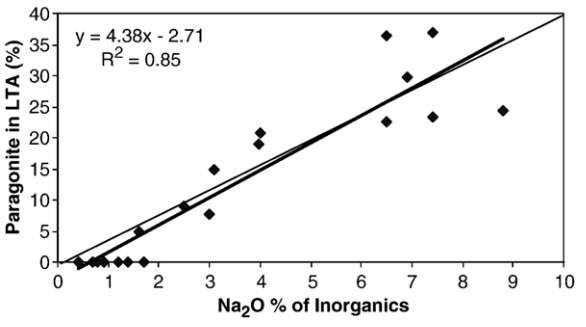


Fig. 9. Correlation between paragonite concentration in LTA and normalised percentage of $Na_2O$ from XRF data.

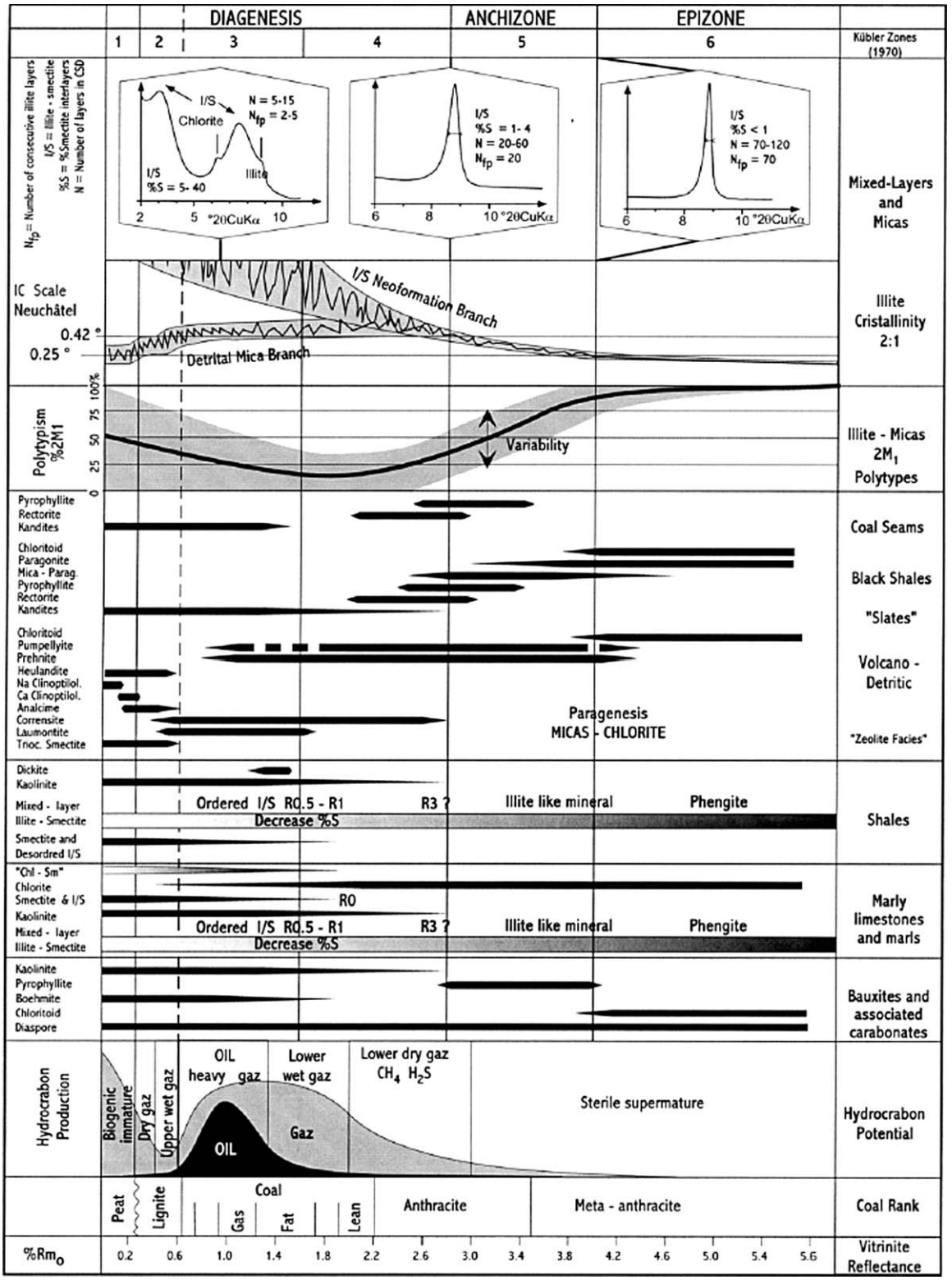


Fig. 10. Relationship between zones of occurrence of metamorphic minerals in relation to vitrinite reflectance and other coal rank indicators (after Kübler and Jaboyedoff, 2000).

Weaver, 1989). Demaison (1974), cited by Weaver (1989), notes that kaolinite associated with coal beds may be destroyed at temperatures of around 150 to 200 °C. However, under low-grade metamorphic conditions in geothermal systems, kaolinite may persist where the reaction is limited by the available time and the chemistry of the environment (Barker et al., 1986).

The disappearance of kaolinite from argilo-detrital shales, based on the Kübler diagram (Fig. 10), can be correlated with a vitrinite reflectance of 1.3–1.4%. Kisch (1987), however, has pointed out that the grade of burial diagenesis at which kaolinite disappears varies significantly in different lithologies, and the mineral is particularly striking through its persistence to anthracite rank in coals, kaolinite–coal tonsteins, and underclays. The stability of kaolinite during burial diagenesis, however, is not only influenced by temperature and pressure but is also determined by wider-ranging geochemical factors (Dunoyer de Segonzac, 1970), such as the availability of other components that allow the reactions to take place.

Kaolinite persists in the coal samples from Bukit Asam to a vitrinite reflectance of 2.2% (Anth-2), but disappears between that level and a reflectance of 4.17% (Table 3). In contrast, kaolinite in the clay partings (Table 4) disappears in samples associated with coal having a vitrinite reflectance of 1.7%.

The differences in kaolinite stability for coal and clay partings may depend on the associated rock composition. It appears that the abundance of organic material favours the persistence of kaolinite in coal at temperatures somewhat higher than those normally expected for kaolinite stability. The persistence of kaolinite at high levels of organic maturation and in close proximity to intrusions may also be influenced by the potassium concentration in the fluid and the duration of its availability (Uysal et al., 2000). A high ratio of $K^+/H^+$ activity in the fluid may cause a decrease in the amount of kaolinite as kaolinite reacts with potassium to form illite or I/S. As discussed further below, this possibility can be extended, in the Bukit Asam deposit, to also include the sodium concentration, and the associated formation of paragonite.

### 4.2. Mixed-layer illite/smectite

The appearance of I/S associated with the disappearance of kaolinite has been reported in many sedimentary basins subjected to burial metamorphism (Kisch, 1983), and mixed-layer clay mineral development has been suggested as a potential indicator of thermal maturation (Smart and Clayton, 1985; Hillier and Clayton, 1989; Uysal et al., 2000). Increasing burial depth has also been associated with a tendency for the mixed-layer clay minerals to be less expandable (e.g. Perry and Hower, 1970; Kisch, 1983; Smart and Clayton, 1985; Chamley, 1989), as well as an increase in ordering and in the overall illite percentage included in the I/S (e.g. Dunoyer de Segonzac, 1970; Kisch, 1987; Uysal et al., 2000). The concentration of I/S may also increase progressively as the distance to the heat source (e.g. intrusion) decreases (Lynch and Reynolds, 1984).

The high proportion of illite and the ordering of the I/S, noted in the high rank coals at Bukit Asam, are consistent with the features of other sediments in the advanced stages of burial metamorphism. A tendency for illitization to increase towards the heat source is noted, for example in the B seam. Sample Anth-2, about 2 m away from the contact and with a vitrinite reflectance of 2.2%, still contains expandable clay minerals, and the I/S in this sample shows a regular ordering towards the rectorite structure. In sample Anth-1 ($Rv_{max}$ = 4.2%), taken about 1 m from the intrusive body, however, no expandable clay is present; the LTA from this sample only contains illite, paragonite and chlorite.

In the absence of other clay minerals in the unmetamorphosed coal or associated claystones, it would appear that the kaolinite in the Bukit Asam beds was the main precursor for the formation of the I/S and the other aluminosilicate minerals. Although it is unusual in other types of sequences for kaolinite to act as the precursor for I/S formation, Frank-Kamenetzky et al. (1971) suggest that, under hydrothermal conditions, at temperatures of around 225 °C and in the presence of KCl, kaolinite may be converted to montmorillonite and disordered kaolinite. At higher temperatures (250 °C) these minerals are converted to K-hydromica, which is the only phase present at temperatures of more than 400 °C. In the presence of NaCl, after conversion to montmorillonite and disordered kaolinite, the kaolinite is converted to Na-hydromica, with a minor proportion of montmorillonite possibly persisting up to a temperature of around 500 °C (Frank-Kamenetzky et al., 1971).

Similar processes appear to have occurred in association with higher-rank coal formation in the Bukit Asam area. Although the lower-rank coals would themselves have had relatively high moisture contents, the highly fractured and faulted structure of the area may have allowed ingress of additional hot fluids in association with thermal metamorphism processes. Such hydrous conditions, in the presence of several key elements (e.g. K, Na, Mg) from the non-mineral inorganics in the low-rank coals, possibly allowed conversion of well-ordered kaolinite to I/S, disordered kaolinite and Na-hydromica (paragonite) at temperatures around 225–250 °C. At deeper horizons the

coal may have experienced even higher temperatures, giving rise to a decrease in the expandable content of the I/S and increasing the illitization and stacking regularity. Mixed-layer clay with less expandability, as well as a rectorite-like I/S mineral, is identified near the bottom of the C seam in the Air Laya area.

Hower et al. (1976) noted that the progressive illitization of I/S with burial (and rank advance) depends in part on the supply of $K^+$ ions to the sediment undergoing metamorphism. The illitization process identified in the present study presumably occurred through such a solid-state transformation, involving substitution of Al for Si with subsequent dehydration and fixation of cations in the smectite interlayers of the I/S. It should be noted, however, that the process requires both aluminium and potassium; the Al in the coals at Bukit Asam may have originated from the breakdown of kaolinite, while the K was probably derived from the inorganic elements in the organic matter of the original low-rank coal seams.

### 4.3. Rectorite-like minerals

Most authors, including Dunoyer de Segonzac (1970), Henderson (1970), Paradis et al. (1983), Kisch (1983) and Frey (1987), have defined rectorite as a highly regular Na-rich mica-type (sodic mica) mixed-layer clay mineral. Chemically, this mineral can be distinguished from ordered K-rectorite (regular K-I/S) by the predominance of sodium over potassium (Kisch, 1983). No chemical data were available in the present study from the actual I/S mineral to confirm the predominance of sodium over potassium, but, as previously mentioned, bulk chemical analysis suggests that sodium is more abundant than potassium in the samples containing an abundance of rectorite-like material.

Many authors (e.g. Sudo et al., 1962; Frey, 1987; Weaver, 1989; Brattli, 1997; Sakharov et al., 1999; Srodon, 1999) indicate that rectorite is restricted to hydrothermal alteration zones and low-grade metamorphic rocks. Rectorite-like clay minerals are further thought to provide evidence of an equilibrium stage during the transformation of irregular I/S under deep diagenesis conditions (Dunoyer de Segonzac, 1970).

Metamorphic aggradation of degraded 2:1 clay minerals essentially involves loss of water, adsorption of $Na^+$, $K^+$ and $Mg^{2+}$, and a rearrangement of ions within the mineral structure (Dunoyer de Segonzac, 1970). During sedimentation and early diagenesis, the transformations are continuous, as the ions incorporated into the sediment are derived from the sedimentary environment and the associated interstitial solutions. In the appropriate chemical conditions, diagenetic aggradation can produce regular mixed-layer structures; for instance, an environment rich in alkali metals may produce a rectorite-like mineral (Dunoyer de Segonzac, 1970).

Pevear et al. (1980) suggested that K-rectorite in bentonite partings of the Tulameen coalfield, British Columbia (Rv = 0.86%), was derived from metamorphism of smectite, sanidine and zeolite. Daniels (1992) suggested kaolinite and smectite as precursors for Na-rectorite formation, while Henderson (1970) suggested pyrophyllite as a possible mediator for the formation of rectorite from kaolinite. Kisch (1987) also noted the relation of K-rectorite to the disappearance of kaolinite in Na-rich shales or slaty black shales at a reflectance value of 0.7–0.9%.

The rectorite-like clay at Bukit Asam first appears in the claystone partings of coal seams with a vitrinite reflectance $\geq 1.3\%$, suggesting a metamorphic origin. It is absent from the lower-rank parts of the deposit, including areas such as Muara Tiga and Banko, where no intrusions are reported.

A metamorphic origin for the rectorite is further confirmed by the mineralogy of the partings in the B seam. A silicified band in the unheated part of this seam (Sample B22, Table 5) consists mainly of kaolinite and quartz, whereas rectorite-like clay dominates an equivalent feature (Sample B26, Table 5) in an area of heated coal with $Rv_{max} = 1.4\%$. Regular mixed-layering with a tendency towards the rectorite structure is also noted in a strongly heated coal sample from the B2 seam (Anth-2, Table 4), taken 2 m from the Suban Sill. In contrast, no rectorite-like structures have been observed in the unheated coals of this seam. A rectorite-like mineral is also identified in a sample of the interburden rock between the B and C seams (Sample BC-2, Table 5) in the heated zone.

The non-coal partings in the unheated C seam (e.g. Samples C16, C19, C21, Table 5) are also dominated by kaolinite, and contain no more than traces of any I/S component. Rectorite-like I/S, however, dominates the partings in the heated coals (Samples C2, C4, C7, Table 5), with no kaolinite apparently being present. Such a dramatic change in mineralogy cannot be explained by depositional features alone, and strongly suggests that the rectorite-like material was formed by metamorphism of the kaolinite in the partings of the unheated coal seam.

The reaction proposed by Daniels (1992) for the formation of Na-rectorite (which he described as mixed-layer paragonite/smectite) in the anthracites of Pennsylvania is probably the best parallel to this relatively uncommon mineralogical system, with the Na-rectorite having formed from a precursor of kaolinite, smectite

or pyrophyllite, through one or more of the following reactions:

$$2\underset{\text{Kaolinite}}{Al_2Si_2O_5(OH)_4} + \underset{\text{Quartz}}{SiO_2} + 0.89Na^+ + 0.11K^+ \rightarrow 1.5(Na_{0.59}K_{0.07})\underset{\text{Rectorite}}{Al_2(Si_{3.33}Al_{0.67})O_{10}(OH)_2} + 2H_2O + H^+ \quad (1)$$

$$1.6(Na_{0.33})\underset{\text{Smectite}}{Al_{1.67}Fe_{0.33}(Si_{3.33}Al_{0.67})O_{10}(OH)_2} + 0.05Na^+ + 0.07K^+ + 0.92H^+ \rightarrow \underset{\text{Rectorite}}{(Na_{0.59}K_{0.07})Al_2(Si_{3.33}Al_{0.67})O_{10}(OH)_2} + 3.07\underset{\text{Quartz}}{SiO_2} + 1.06H_2O + 0.54Fe^{2+} \quad (2)$$

$$2\underset{\text{Pyrophyllite}}{Al_2Si_4O_{10}(OH)_2} + 0.89Na^+ + 0.11K^+ \rightarrow 1.5\underset{\text{Rectorite}}{(Na_{0.59}K_{0.07})Al_2(Si_{3.33}A_{1.67})O_{10}(OH)_2} + 3\underset{\text{Quartz}}{SiO_2} + H^+ \quad (3)$$

Because smectite and pyrophyllite were not observed in the present study, and kaolinite and quartz are the dominant minerals in the partings of the lower-rank areas (Table 5), the most likely precursors for the formation of the rectorite-like clay at Bukit Asam are kaolinite and quartz, following reaction (1) above. Furthermore, as the reactions involve both potassium and sodium, the final product, i.e. whether it is K-rectorite or Na-rectorite, will depend on the dominant cation available in the fluid of the associated rocks. Since the chemistry of the relevant rocks in the study area suggests that sodium is more abundant than potassium, it is even more likely that reaction (1) was the main process that formed the rectorite-like clay in the Bukit Asam area.

Several studies have provided direct or indirect estimates of temperature for the formation of rectorite. Daniels (1992) and Paradis et al. (1983) considered the temperature for the formation of Na-rectorite to be 225–275 °C, whereas vitrinite reflectance data for K-rectorite in non-coal beds (Rv=0.86%), as observed by Pevear et al (1980), suggest a minimum temperature of 145–160 °C. Eslinger and Savin (1976) have identified rectorite-like mixed-layer minerals in hydrothermal areas at measured borehole temperatures of 220–270 °C, while Steiner (1968) noted the formation of a rectorite-like mineral at about 200 °C.

The vitrinite reflectance of 1.3–1.7% for the coal associated with the rectorite-like clays at Bukit Asam indicates that development of the clays may have begun at a temperature somewhat higher than 160 °C. However, as the regional rank of Bukit Asam coal corresponds to a vitrinite reflectance of 0.3–0.4% and limited samples are available with a reflectance between 0.7% and 1.3%, the rank and temperature initiating the rectorite-like development might also have been somewhat lower.

Where data are available on a ply-by-ply basis, the stacking regularity resembling rectorite is only recognised in the coals near the base of the C seam, and is not observed in the other coals of the same seam section (Table 4). In contrast, rectorite-like clay is present in all of the non-coal rocks in the seam section (Table 5), including the roof and floor rocks as well as the intra-seam claystone partings.

The primary controls on the formation of ordered I/S, apart from temperature and time, are rock composition, permeability and fluid chemistry (Hillier and Clayton, 1989; Brattli, 1997; Uysal et al., 2000). Differences in rock composition and fluid chemistry between the coal and the non-coal rocks may therefore have influenced the degree of ordering of the I/S in both materials. Fractures in the coal could have provided sufficient permeability to allow circulation of neutral solutions with relatively high $K^+ / H^+$ activity ratios. On the other hand, the inorganic partings may have had lower water / rock ratios and only limited potassium supply, reducing the degree of illitization and limiting the ordering of the I/S to $R=1$, without the capacity to reach the higher degree of ordering ($R=3$) found in the I/S of the coal samples.

### 4.4. Paragonite-bearing assemblages

Paragonite is found only in the heat-affected coals at Bukit Asam, and thus thermal metamorphism, combined with favourable coal chemistry, apparently provided suitable conditions for paragonite development. According to Zen (1960), paragonite may be formed through the following reaction:

$$\underset{\text{Albite}}{Na_2AlSi_3O_8} + \underset{\text{Kaolinite}}{Al_2(Si_2O_5(OH)_4)} \leftrightarrow \underset{\text{Paragonite}}{NaAl_2(AlSi_3)O_{10}(OH)_2} + 2\underset{\text{Quartz}}{SiO_2} + H_2O$$

However, thermodynamic calculations indicate that this reaction is metastable at low temperature (<120 °C) and low pressure ($P<500$ kbar), and is unlikely to occur in nature (Frey, 1987).

Another reaction for paragonite formation from a precursor of Na montmorillonite was proposed by Chatterjee (1973), based on hydrothermal experiments:

$$\underset{\text{Na-montmorillonite}}{3Na_{0.33}Al_2(Al_{0.33}Si_{3.67})O_{10}(OH)_2} + \underset{\text{Albite}}{2Na_2AlSi_3O_8} \leftrightarrow \underset{\text{Paragonite}}{NaAl_2(AlSi_3)O_{10}(OH)2} + \underset{\text{Quartz}}{8SiO_2}$$

The associated laboratory experiments indicated a temperature of about 315–325 °C and a pressure of 2–7 kbar for this reaction. Similar experiments by Hemley and Jones (1964) and Althaus and Johannes (1969) indicated a temperature slightly above 300 °C. As the experiments were not reversed, a somewhat lower temperature may be expected in nature (Frey, 1987).

Since Na-montmorillonite was not observed in the present study, and kaolinite is the dominant clay mineral in the unheated coals, kaolinite is thought to have been the ultimate precursor for paragonite formation at Bukit Asam. In the absence of albite or other Na-bearing minerals, the Na for the reaction was presumably derived from the inorganic elements associated with the coal's organic matter.

Paragonite is also more abundant in the coal samples at Bukit Asam than the inorganic partings and roof/floor rocks (Tables 4 and 5). Chemical analysis indicates that the concentration of $Na_2O$ in the coal samples (Table 6), including both heated and unheated coals, is considerably higher than in the associated non-coal rocks, especially if computed to a mineral-matter-only basis. The abundance of $Na_2O$ in the lower-rank coal samples, and the absence of Na-rich minerals from the corresponding LTAs, suggests that most of sodium was originally present as an organically associated inorganic element or in the coal's pore water (cf. Ward, 1991; 2002). In the higher-rank coals, as indicated by Fig. 9, the abundant Na is represented by the paragonite component.

The lowest-rank coal samples at Bukit Asam containing paragonite have a vitrinite reflectance of 1.4%, much lower than the vitrinite reflectance of around 2.2% suggested for paragonite formation in Kübler's diagram (Fig. 10). This may indicate that the temperature (and perhaps also the pressure) for the paragonite formation in a particular area is additionally be determined by geochemical controls from the minerals and/or fluids present, leading in turn to temperatures less than those commonly accepted for paragonite formation.

### *4.5. Role of non-mineral inorganic elements*

The results of this study suggest that almost all of the reactions leading to the formation of new minerals (illite/smectite, rectorite and paragonite) in the high rank coals at Bukit Asam involved the non-mineral inorganic elements in the coal as an inherent part of the process. Ward (2002) and Ward et al. (2003) have suggested that expulsion of moisture (along with any associated materials in solution) and changes in the chemical structure of the organic matter may combine to remove the non-mineral inorganics from coal with rank advance, and if these constituents still persist in higher rank coals, they are typically present only in relatively minor proportions.

Artefact minerals derived from the non-mineral inorganics still persist in significant concentrations (average 10.3%) in the LTA of the higher-rank coals at Bukit Asam (Table 3). The overall proportion of artefacts is nevertheless about half of their average concentration in the LTA of the lower-rank coal samples. Some of the sulphates grouped with these artefacts, moreover (e.g. jarosite and coquimbite), may also represent oxidation products of pyrite in the original coal material.

Reactions involving at least some of the non-mineral inorganic elements, such as Na, may be responsible for the formation of the new minerals, such as paragonite, in the heated coals at Bukit Asam. Indeed, the presence of such elements, due to the low rank of the coal when intrusion took place, is probably a fundamental reason why the reactions occurred. It also serves to distinguish the mineralogical metamorphism of the Bukit Asam coals and associated non-coal beds from the changes developed with the more protracted rank increases associated with burial processes, or derived from intrusions into coals that were already at higher rank levels.

## 5. Conclusions

The rank of the coal in parts of the Bukit Asam deposit has been increased from regional sub-bituminous levels ($Rv_{max}$ = 0.45%) to that of bituminous coal and anthracite ($Rv_{max}$ up to at least 4%) by localised heat flow from nearby igneous intrusions. In addition to affecting the properties of the organic matter, the metamorphism has brought about significant changes in the mineralogy of the coal and associated non-coal beds.

The localised increases in temperature associated with the intrusion appear to have metamorphosed some minerals in the original coal, especially kaolinite, into new phyllosilicate phases. The heating may have remobilised some of the moisture and associated inorganic elements in the low-rank coal, or introduced new hot liquids into the coal-bearing formation, providing elements that also became involved in the reactions with the original mineral components.

Kaolinite, which is the dominant mineral in the lower-rank coals, decreases in abundance and even disappears in the higher-rank coals. There is also a change in the kaolinite structure, from well ordered in the low rank coals to poorly ordered in the high rank coal samples. Kaolinite persists in coal samples up to a vitrinite reflectance of around 2.2%, but disappears between that level and a vitrinite reflectance of 4.2%. Mixed-layer I/S, which occurs in no more than trace amounts in the lower-rank coals, increases to become the dominant mineral in the higher-rank coal samples. The degree of illitization of the I/S also tends to increase, especially towards the contacts with the intrusive bodies.

Paragonite and rectorite-like I/S, which are totally absent from the unheated or slightly heated coals, become major minerals in the heated coal seams. The clay partings in the heated or slightly heated areas ($Rv_{max}$ <1%) are dominated by kaolinite, but kaolinite is absent from the clay partings in the heated coal areas and the intra-seam bands become dominated by rectorite-like clay minerals. Paragonite likewise becomes abundant in the coals themselves, especially in the heated C seam materials.

The mineralogical changes at Bukit Asam appear to reflect interaction of the kaolinite in the original lower-rank coal and intra-seam bands with elements such as K and Na, which were present as non-mineral inorganics in the unmetamorphosed coal beds. Consideration of the various models for formation of these minerals provide a firmer basis for understanding the changes that have taken place, and show that many of the reactions and mineral products are similar to those associated with metamorphism or thermal alteration of other sedimentary strata. This similarity, however, is brought about be the presence of the key inorganic elements in the coals at Bukit Asam, due to the low rank of the coals at the time they were affected by the intrusive bodies. Such changes do not appear to occur in the more protracted metamorphism (rank advance) due to coal seam burial, where the non-mineral inorganics may progressively escape from the organic matter before the relevant temperatures are reached, nor with igneous intrusions into higher-rank coals, where the non-mineral inorganics would have already been driven out of the intruded coal bed.

## Acknowledgements

Thanks are expressed to the Australian Development Scholarship Program for financial support to pursue this study, and to Perusahaan Tambang Batubara Bukit Asam for their generous assistance with the field work. Thanks are also expressed to Rad Flossman, Irene Wainwright, Ervin Slansky, Zhongsheng Li, Dorothy Yu and Vera Piegerova, for their assistance with sample preparation, instrument operation, XRD interpretation and electron microscope analysis, and to the referees for their constructive comments.

## References

Althaus, E., Johannes, W., 1969. Experimental metamorphism of NaCl-bearing aqueous solutions by reactions with silicates. American Journal of Science 267, 87–98.

Barker, C.E., Crysdale, B.L., Pawlewicz, M.J., 1986. The relationship between vitrinite reflectance, metamorphic grade, and temperature in the Cerro Prieto, Salton Sea and East Mesa geothermal systems, Salton Trough, United States and Mexico. In: Mumpton, F.A. (Ed.), Studies in Diagenesis. U.S Geological Survey Bulletin, vol. 1578, pp. 83–95.

Brattli, B., 1997. A rectorite–pyrophyllite–chlorite–illite assemblage in pelitic rocks from Colombia. Clay Minerals 32, 425–434.

Chamley, H., 1989. Clay Sedimentology. Springer-Verlag, Berlin. 623 pp.

Chatterjee, N.D., 1973. Low-temperature compatibility relations of the assemblage quartz–paragonite and the thermodynamic of the phase rectorite. Contributions to Mineralogy and Petrology 42, 259–271.

Daniels, E.J., 1992. Nature and origin of minerals in anthracite from eastern Pennsylvania. Ph.D. Thesis, University of Illinois, Urbana-Champaign.

Daniels, E.J., Aronson, J.L., Altaner, S.P., Clauer, N., 1994. Late Permian age of $NH_4$-bearing illite in anthracite from Eastern Pennsylvania: temporal limits on coalification in the Central Appalachians. Geological Society of America Bulletin 106 (6), 760–766.

Daulay, B., 1985. Petrology of some Indonesian and Australian Tertiary coals. Unpublished M.Sc. (Hons) thesis, University of Wollongong, Australia, 256 pp.

Daulay, B., Cook, A.C., 1988. The petrology of some Indonesian coals. Journal of Southeast Asian Earth Sciences 2 (2), 45–64.

de Coster, G.L., 1974. The geology of the Central and South Sumatra basins. Indonesian Petroleum Association, 3rd Annual Convention, pp. 77–110.

Demaison, G.J., 1974. Relationship of coal rank to paleotemperatures in sedimentary rocks. In: Alpern, B. (Ed.), Petrographiede la matiere organique des sediments, relations avec la paleotemperature et le potential petrolier. Coll. Int. Symposium, vol. 1973. CNRS, Paris, pp. 217–224.

Dunoyer de Segonzac, G., 1970. The transformation of clay minerals during diagenesis and low grade metamorphism, a review. Sedimentology 15, 281–346.

Eslinger, E.V., Savin, S.M., 1976. Mineralogy and $O^{18}/O^{16}$ ratios of the fine-grained quartz and clay from site 323. In: Worstell, P. (Ed.), Initial Reports on the Deep Sea Project, Leg, vol. 35. U.S Government Printing Office, Washington, D.C, pp. 489–496.

Frank-Kamenetzky, V.A., Kotov, N.V., Goilo, E.A., Klotchkova, G.N., 1971. Structural transformation of some clay minerals under pressure in hydrothermal conditions. International Mineralogical Association, 7th General Meeting, Papers and Proceedings; special paper. Mineralogical Society of Japan 1, 88–97.

Frey, M., 1970. The step from diagenesis to metamorphism in pelitic rocks during Alpine orogenesis. Sedimentology 15 (3–4), 261–279.

Frey, M., 1978. Progressive low-grade metamorphism of a black shale formation, central Swiss Alps, with special reference to

pyrophyllite and margarite bearing assemblages. Journal of Petrology 19 (1), 95–135.
Frey, M., 1987. Very low grade metamorphism of clastic sedimentary rocks. In: Frey, M. (Ed.), Low-temperature Metamorphism. Blackie and Sons, Glasgow, pp. 9–58.
Griffin, G.M., 1971. Interpretation of X-ray diffraction data. In: Carver, R.E. (Ed.), Procedures in Sedimentary Petrology. John Wiley and Sons, New York, pp. 541–569.
Haan, E.J., 1976. Stratigraphy and structure of the coal deposits surrounding the Taba concession, South Sumatra. Shell Minjbouw, 19 pp.
Hemley, J.J., Jones, W.R., 1964. Chemical aspects of hydrothermal alteration with emphasis on hydrogen metasomatism. Economic Geology 59, 539–567.
Henderson, G.V., 1970. The origin of pyrophyllite rectorite in shales of North Central Utah. Clays and Clay Minerals 18, 239–246.
Hillier, S., Clayton, T., 1989. Illite/smectite diagenesis in Devonian lacustrine mudrocks from northern Scotland and its relationship to organic maturity indicators. Clay Minerals 24 (2), 181–196.
Hower, J., Eslinger, W.V., Hower, M., Perry, E.A., 1976. Mechanism of burial metamorphism of argillaceous sediments: I. Mineralogical and chemical evidence. Geological Society of America Bulletin 87, 725–737.
Hutchison, C.S., 1989. Geological Evolution of Southeast Asia. Oxford University Press, New York. 333 pp.
Kisch, H.J., 1983. Mineralogy and petrology of burial diagenesis (burial metamorphism) and incipient metamorphism in clastic rocks. In: Larsen, G., Chilingar, G.V. (Eds.), Diagenesis in Sediments and Sedimentary Rocks. Developments in Sedimentology, vol. 2. Elsevier, Amsterdam, pp. 289–494.
Kisch, H.J., 1987. Correlation between indicators of very low grade metamorphism. In: Frey, M. (Ed.), Low Temperature Metamorphism. Blackie and Sons, Glasgow, pp. 207–304.
Kisch, H.J., Taylor, G.H., 1966. Metamorphism and alteration near an intrusive-coal contact. Economic Geology 61, 343–361.
Kübler, B., Jaboyedoff, M., 2000. Illite crystallinity: concise review paper. Comptes Rendus de l'Academie des Sciences, Serie II, Sciences de la Terre et des Planetes (Earth and Planetary Sciences) 331 (2), 75–89.
Kwiecinska, B.K., Hamburg, G., Vleeskens, J.M., 1992. Formation temperatures of natural coke in the Lower Silesian coal basin, Poland: evidence from pyrite and clays by SEM-EDX. International Journal of Coal Geology 21, 217–235.
Lynch, L., Reynolds Jr., R.C., 1984. The stoichiometry of the smectite–illite fraction. Program and Abstracts, 21st Annual Conference, Clay Minerals Society, Baton Rouge, Louisiana, Sept 30–Oct 3, 1984. 8 pp.
Matasak, Th., Kendarsi, R., 1980. Geologi endapan batubara di Bukit Asam — Sumatra Selatan, Buletin Departemen Geologi. Institut Teknologi Bandung 1, 11–33.
Miller, R.N., Given, P.H., 1978. A geochemical study of the inorganic constituents of some low-rank coals. Report, Contract EX-76-C-01-2494, U.S. Department of Energy, Coal Research Section, Pennsylvania State University: 314 pp.
Miller, P.N., Yarzab, R.F., Given, P.H., 1979. Determination of mineral matter content of coals by low -temperature ashing. Fuel 58, 4–10.
Moore, D.M., Reynolds Jr., R.C., 1997. X-ray Diffraction and the Identification and Analysis of Clay Minerals, 2nd Ed. Oxford University Press, Oxford. 378 pp.
Norrish, K., Chappell, B.W., 1977. X-ray fluorescence spectrometry. In: Zussman, J. (Ed.), Physical Methods in Determinative Mineralogy. Academic Press, London, pp. 201–272.
Paradis, S., Velde, B., Nicot, E., 1983. Chloritoid–phyrophyllite–rectorite facies rocks from Brittany, France. Contributions to Mineralogy and Petrology 83 (3–4), 342–347.
Perry, E.D., Hower, J., 1970. Burial diagenesis in Gulf Coast pelitic sediments. Clays and Clay Minerals 18, 165–177.
Pevear, D.R., Williams, V.E., Mustoe, G.E., 1980. Kaolinite, smectite, and K-rectorite in bentonites; relation to coal rank at Tulameen, British Columbia. Clays and Clay Minerals 28 (4), 241–254.
Pujobroto, A., 1997. Organic petrology and geochemistry of Bukit Asam coal, South Sumatra, Indonesia. Unpublished Ph.D. thesis, University of Wollongong, Australia, 397 pp.
Rao, C.P., Gluskoter, H.J., 1973. Occurrence and distribution of minerals in Illinois coals. Illinois State Geological Survey Circular 476 (56 pp.).
Renton, J.J., 1982. Mineral matter in coal. In: Meyers, R.A. (Ed.), Coal Structure. Academic Press, New York, pp. 283–325.
Ruan, C.D., Ward, C.R., 2002. Quantitative X-ray powder diffraction analysis of clay minerals in Australian coals using Rietveld methods. Applied Clay Science 21, 227–240.
Sakharov, B.A., Lindgreen, H., Salyn, A., Drits, V.A., 1999. Determination of illite/smectite structures using multi-specimen X-ray diffraction profile fitting. Clays and Clay Minerals 47 (5), 555–566.
Sanguesa, F.J., Arostegui, J., Suarez-Ruiz, I., 2000. Distribution and origin of clay minerals in the Lower Cretaceous of the Alava Block (Basque–Cantabrian Basin Spain). Clay Minerals 35, 393–410.
Sarangih, C., 1985. Mikropetrographische untersuchungen an braunkohlen aus der bohrung GHL7 Bukit Asam, Sumatra, Indonesien. Diplomarbeit R.W.T.H-Aachen. 56 pp.
Shell Minjbouw, N.V., 1978. Explanatory notes to the geological map of the South Sumatran Coal Province. 31 pp.
Smart, G., Clayton, T., 1985. The progressive illitization of interstratified illite–smectite from Carboniferous sediments of northern England and its relationship to organic maturity indicators. Clay Minerals 20, 455–466.
Srodon, J., 1999. Nature of mixed-layer clays and mechanism of their formation and alteration. Annual Review of Earth and Planetary Sciences 27, 19–53.
Stalder, P., 1971. Die Kaolin-Kohlentonsteine aus dem Westfal C und B der Untertagebohrung 150 der Steinkohlenbergwerke Ibbenüren und ihre Bedeutung für die Karbonstratigraphie Nordwestdeutschlands. Fortschrifte Geologisches Rheinland Westfalen 18, 79–100.
Stalder, P., 1976. A Review of the South Sumatra Coal Basin, Shell Minjbuow, N.V. Jakarta.
Standards Australia, 2000. Higher rank coal — mineral matter and water of constitution. Australian Standard 1038 Part 22. 20 pp.
Steiner, A., 1968. Clay minerals in hydrothermally altered rocks at Waireki, vol. 16. Clays and Clay Minerals, New Zealand, pp. 193–213.
Sudo, T., Hayashi, H., Shimoda, S., 1962. Mineralogical problems of intermediate clay minerals. Clays Clay Minerals, Proceedings of 9th National Conference on Clays and Clay Minerals, 1960, pp. 378–392.
Susilawati, R., 2004. Minerals and Inorganic Matter in Coals of the Bukit Asam Coalfield, South Sumatra Basin, Indonesia. Unpublished M.Sc. thesis, University of New South Wales, Australia, 224 pp.
Sykes, R., Lindqvist, J.K., 1993. Diagenetic quartz and amorphous silica in New Zealand coals. Organic Geochemistry 20 (6), 855–866.
Taylor, J.C., 1991. Computer programs for standardless quantitative analysis of minerals using the full powder diffraction profile. Powder Diffraction 6, 2–9.

Uysal, I.T., Glikson, M., Golding, S.D., Audsley, F., 2000. The thermal history of the Bowen Basin, Queensland, Australia: vitrinite reflectance and clay mineralogy of late Permian Coal Measures. Tectonophysics 323 (1–2), 105–129.

Velde, B., 1985. Clay Minerals: A Physico-Chemical Explanation of their Occurrence. Elsevier, Amsterdam. 427 pp.

Waluyo, B.H., 1992. The assessment of Banko Barat coal of South Sumatra as a fuel for the Suralaya steam power electric generating plant. MSc Thesis, University of Wollongong, Australia, 123 pp.

Ward, C.R., 1991. Mineral matter in low-rank coals and associated strata of the Mae Moh Basin, northern Thailand. International Journal of Coal Geology 17, 69–93.

Ward, C.R., 1992. Mineral matter in Triassic and Tertiary low-rank coals from South Australia. International Journal of Coal Geology 20, 185–208.

Ward, C.R., 2002. Analysis and significance of mineral matter in coal seams. International Journal of Coal Geology 50, 135–168.

Ward, C.R., Warbrooke, P.R., Roberts, F.I., 1989. Geochemical and mineralogical changes in a coal seam due to contact metamorphism, Sydney Basin, New South Wales, Australia. International Journal of Coal Geology 11, 105–125.

Ward, C.R., Spears, D.A., Booth, C.A., Staton, I., Gurba, L.W., 1999. Mineral matter and trace elements in coals of the Gunnedah Basin, New South Wales, Australia. International Journal of Coal Geology 40, 281–308.

Ward, C.R., Gurba, L.W., Li, Z., Susilawati, R., 2003. Distribution of inorganic elements in lower-rank coal macerals as indicated by electron microprobe techniques. Proceedings of 12th International Conference on Coal Science, Cairns Queensland, 2–6 November. 10 pp. (CD publication).

Weaver, C.E., Broekstra, B.E., 1984. Illite–Mica. In: Weaver, C.E. (Ed.), Shale–slate metamorphism in the Southern Appalachians. Elsevier, Amsterdam, pp. 67–97.

Weaver, C.E., 1989. Clays, Muds and Shales. Developments in Sedimentology, vol. 44. Elsevier, Amsterdam. 819 pp.

Zen, E., 1960. Metamorphism of lower Paleozoic rocks in the vicinity of the Taconic Range in West Central Vermont. American Mineralogist 45, 129–175.